Technische Universität München
Wissenschaftszentrum Weihenstephan für Ernährung, Landnutzung und Umwelt
Lehrstuhl für Bodenkunde

Soil microaggregation and microspatial patterns of organic matter accrual

Steffen Adrian Schweizer

Vollständiger Abdruck der von der Fakultät Wissenschaftszentrum Weihenstephan für Ernährung, Landnutzung und Umwelt der Technischen Universität München zur Erlangung des akademischen Grades eines

Doktors der Naturwissenschaften

genehmigten Dissertation.

Vorsitzender:		Prof. Dr. Johan Philipp Benz
Prüfer der Dissertation:	1.	Prof. Dr. Ingrid Kögel-Knabner
	2.	Prof. Dr. Georg Guggenberger
	3.	Assoc. Prof. Dr. Peter Kopittke

Die Dissertation wurde am 30.01.2020 bei der Technischen Universität München eingereicht und durch die Fakultät Wissenschaftszentrum Weihenstephan am 26.05.2020 angenommen.

Für Anna, Theo und Flora.

„Our imagination is struck only by what is great;
but the lover of natural philosophy should reflect equally on little things.“

Alexander von Humboldt (1769–1859)

I Summary

Soil microaggregates control essential soil processes such as organic matter (OM) turnover and storage in structural entities with a diameter <250 μm, which hold a long-term storage potential. Despite evidence for the important role of fine mineral particles, the relations between the arrangement of organo-mineral associations at the microscale and the sequestration of OM in microaggregates are not clear. This work aimed to resolve microspatial patterns of mineral-associated OM, determine whether fine mineral particles influence the distribution and arrangement of OM and investigate how soil texture alters microaggregate diameters, which could mediate OM concentrations. These objectives were approached with a glacier chronosequence and an arable field site with a clay content gradient. The study sites were analyzed using combined density and particle size fractionations and by isolating microaggregate-sized fractions. Spatially resolved techniques provided measures of the arrangement of OM and mineral surfaces at the microscale in soils.

The initial soil formation in clay-sized soil fractions along a chronosequence in the forefield of the retreating Damma glacier (Switzerland) was investigated in Study I. A novel image analysis protocol was developed to segment mineral surface and OM patches based on elemental distributions measured by nanoscale secondary ion mass spectrometry (NanoSIMS). This enabled to quantify spatial patterns of initially forming soil microaggregates as governed by the accrual of OM over time: Successive microspatial patterns revealed a development of discrete patches to more connected OM structures. Despite the continuous accrual of OM over time, the mineral surface was not completely covered. The C and N composition of the OM patches reflected the postulated ecological development of initially decreasing C:N ratios and increasing C:N ratios at later stages. The results of this study provide direct evidence that carbon sequestration drives the development of OM patches at the microscale that is mostly decoupled from mineral surface area, so that it retains the surface area partly for other soil functions.

The influence of fine mineral particles on OM sequestration was analyzed in Study II using a clay content gradient (5–37 %) sampled from an agricultural research site in Scheyern (Germany). A combined density and size fractionation provided insights into the distribution of OM within particulate and differently sized mineral-associated fractions. Although the soils contained similar concentrations of OM in the bulk soil, the organic carbon (OC) concentrations in the density fractions indicated a change of OM sequestration mechanisms in soils with lower clay content (<18 %) compared to soils with higher clay content (>18 %). The high-clay soils, which contained more mineral surface area that could potentially associate directly with OM, were rather related with increasing proportions of occluded particulate OM

instead of more mineral-associated OM. In the low-clay soils, the OC concentrations in all fine mineral-associated fractions were found to increase with lower clay contents. To determine whether this change of OC concentrations also affects the arrangement of OM at the microscale, N_2-sorption was used to determine the mineral surface area associated with OM through OM removal by NaOCl. This approach revealed that the specific surface area of mineral-associated OM remained constant in the fine silt-sized fraction and the coarse-clay sized fraction despite higher OC concentrations. A similar result was obtained using the spatial analysis of the elemental distribution at the microscale, which was developed in Study I. Accordingly, the higher and more concentrated amount of mineral-associated OC in the low-clay soils was concluded to be arranged in piled-up OM assemblages. The arrangement of OM in such voluminous assemblages explains why OM sequestration is decoupled from the mineral surface area which, therefore, does not pose a limiting factor for the potential of OC accrual.

The interactions between different soil primary particle and microaggregate size distributions were examined in Study III using the high-clay soils of the clay content gradient of 16–37 % from the agricultural research site in Scheyern. A novel approach using dynamic image analysis enabled to differentiate the size composition of aggregates, aggregated particles and unaggregated particles within wet-sieved free size fractions and wet-sieved and sonicated occluded size fractions <250 μm. This provided information about the preferential size range of microaggregates, which was found to be approximately 30 μm independent of the clay content. However, more macroaggregates >250 μm and larger microaggregates in the 50–180 μm size range were found in soils with higher clay content. In turn, the buildup of larger aggregates might have been impeded by higher proportions of sand grains >100 μm in soils containing lower clay content. The wet-sieved size fraction >250 μm was found to contain 4 % more clay-sized particles across the whole clay content gradient, which might be required to stabilize these larger macroaggregates. The small size fraction <53 μm contained higher OC concentrations than the size fraction 53–250 μm, especially in the soils with lower clay contents. Despite these differences in OC concentrations, the OM composition in fractions did not differ between soils from different clay contents but between the size fractions as indicated by lower alkyl:O/N-alkyl ratios in the fraction 53–250 μm by ^{13}C nuclear magnetic resonance spectroscopy. The effect of soil texture was concluded to predominantly stabilize larger and more aggregates, which indirectly contributes to OM sequestration.

Different failure mechanisms of soil microaggregates, like dispersion or breakdown, and their relation with aggregate properties were investigated in Study IV by comparing aggregate isolation methods. A newly developed method was used to mechanically isolate microaggregate-sized fractions by uniaxial dry crushing from soils of the agricultural research

site in Scheyern. In comparison with wet-sieved samples, the dry-crushed fractions exhibited a higher mechanical stability and bacterial diversity. This was intimately related with different failure mechanisms and particle size composition depending on the isolation method. Dry-crushed microaggregates were larger and contained more sand-sized particles, whereas the sand-sized particles were dispersed after wetting. This led to smaller microaggregates, which contained more fine particles than the dry-crushed microaggregates. To investigate the effect of different soil textures on microaggregate sizes, soils with different clay contents were compared (19 %, 24 % and 34 %). According to dynamic image analysis, the dry-crushed microaggregates were found to be of up to 40 μm larger diameters due to more sand-sized particles in the aggregates. These sand-sized particles also led to a dilution of the OC concentration in the dry-crushed size fraction 53–250 μm with decreasing clay content. The effect of the isolation method on microaggregate sizes and properties implies that dry crushing is a useful alternative to wet sieving, when aggregates including sand-sized particles need to be preserved.

Overall, the results of this work revealed distinct spatial patterns that drive the OM sequestration in soil microaggregates. Both Studies I and II show that OM sequestration is consolidated to specific mineral surface sites in fine mineral particle fractions. However, OM sequestration through partial surface coverage and the three-dimensional extension of the proportion of OM-covered surface area indicate that the sequestration of OM is largely decoupled from mineral surface area, where OM accrual may be initiated but not limited by the availability of mineral surface. Instead, the piled-up arrangement of OM provides an independent conception for the potential of soils to sequester OC. At the scale of microaggregates, fine mineral particles stabilized larger aggregates in wet-sieved fractions and more occluded particulate OM in soils with increasing clay content in Studies II and III. The comparisons of microaggregate isolation methods in Study IV demonstrated that sand-sized particles are part of dry-crushed aggregates but dispersed after wetting, which influences correlations with OM concentrations. These findings shows how soil texture indirectly affects OM sequestration via the formation of aggregate architectures that stabilize OM but also sand-sized particles. The results of this work provide evidence for spatially resolved interactions that drive the sequestration of OM in soils at the microscale of mineral surfaces and microaggregates.

II Zusammenfassung

Bodenmikroaggregate beeinflussen entscheidende Bodenprozesse wie die Umsetzung organischer Bodensubstanz (OBS) und deren Einlagerung in Struktureinheiten mit einem Durchmesser von <250 μm, in denen OBS über einen relativ langen Zeitraum überdauern kann. Trotz Hinweisen auf die wichtige Rolle feiner Mineralpartikel, sind die Zusammenhänge zwischen der Anordnung organo-mineralischer Assoziationen auf der Mikroskala und der Ansammlung von OBS in Mikroaggregaten unklar. Diese Arbeit zielt ab auf ein besseres Verständnis mikroräumlicher Verteilungsmuster von mineral-assoziierter OBS, die Feststellung ob feine Mineralpartikel die Verteilung und Anordnung von OBS verändern können und die Untersuchung wie die Bodentextur den Durchmesser von Mikroaggregaten beeinflusst, was die Konzentrationen von OBS beeinträchtigen könnte. Diese Zielsetzungen wurden mithilfe einer glazialen Chronosequenz und einem Ackerstandort mit Tongehaltsgradienten umgesetzt. Die Untersuchungsflächen wurden anhand einer kombinierten Dichte- und Partikelgrößen-fraktionierung sowie mittels der Gewinnung von Größenfraktionen in der Größenordnung von Mikroaggregaten analysiert. Räumlich aufgelöste Techniken stellten Messungen auf der Mikroskala zur Verfügung, um die Anordnung von OBS und Mineraloberflächen zu quantifizieren.

Die anfängliche Bodenbildung in den tongroßen Bodenfraktionen einer Chronosequenz im Vorfeld des Dammagletschers (Schweiz) wurde in Studie I untersucht. Eine neuartige Bildanalyse wurde entwickelt, um Mineraloberflächen und OBS Patches auf der Grundlage von Elementverteilungen gemäß Nano Sekundärionen-Massenspektrometrie (NanoSIMS) zu segmentieren. Dies ermöglichte es räumliche Verteilungsmuster bei der Neubildung von Bodenmikroaggregaten quantitativ zu erfassen, welche stark von der Ansammlung von OBS über die Zeit bestimmt wurden: Sukzessive mikroräumliche Verteilungsmuster zeigten die Entwicklung von diskreten Patches zu mehr verbundenen OBS Strukturen. Trotz kontinuierlicher Ansammlung von OBS über die Zeit war die Mineraloberfläche nicht komplett bedeckt. Die Zusammensetzung der OBS Patches aus C und N spiegelt die früher postulierte ökologische Entwicklungsreihe wider, mit anfänglich abfallenden C:N Verhältnissen und ansteigenden C:N Verhältnissen im späteren Verlauf. Die Ergebnisse dieser Studie geben einen unmittelbaren Nachweis wie die Ansammlung von Kohlenstoff die Entwicklung von OBS Patches auf der Mikroskala antreibt, welche größtenteils von der Größe der Mineraloberfläche entkoppelt sind und so teilweise für anderen Bodenfunktionen beibehalten wird.

Der Einfluss feiner Mineralpartikel auf die Ansammlung von OBS wurde in Studie II untersucht mittels eines Tongehaltsgradienten (5–37 %) innerhalb einer landwirtschaftlichen

Forschungsstation in Scheyern (Deutschland). Eine kombinierte Dichte- und Partikelgrößenfraktionierung gewährte Einblicke in die Verteilung von OBS in partikulären und verschieden großen mineral-assoziierten Fraktionen. Obwohl die Böden ähnliche OBS Konzentrationen im Gesamtboden enthielten, zeigte die Verteilung des organischen Kohlenstoffs (C_{org}) in den Dichtefraktionen eine mechanistische Veränderung der OBS Ansammlung zwischen Böden mit niedrigem Tongehalt (<18 %) und Böden mit hohem Tongehalt (>18 %) an. Die tonreicheren Böden, welche mehr Mineraloberfläche enthielten die potentiell direkt mit OBS assoziieren könnte, wiesen eher höhere Anteile okkludierter partikulärer OBS auf statt mehr mineral-assoziierter OBS. In den tonärmeren Böden wurde festgestellt, dass die C_{org} Konzentrationen in allen feinen mineral-assoziierten Fraktionen anstiegen in Böden mit niedrigerem Tongehalt. Um festzustellen, ob dieser Wandel der C_{org} Konzentrationen sich auch auf die Anordnung von OBS auf der Mikroskala auswirkt, wurde die Größe der Mineraloberfläche, die mit OBS assoziiert ist, mithilfe der Sorption von N_2 und der Entfernung der OBS durch NaOCl ermittelt. Diese Vorgehensweise zeigt auf, dass die spezifische Oberfläche der mineral-assoziierten OBS in der Feinschluff- und der Grobtonfraktion konstant blieb trotz höherer C_{org} Gehalte. Ein ähnliches Ergebnis wurde auch durch die räumliche Untersuchung der Elementverteilung auf der Mikroskala erhalten, welche in Studie I entwickelt wurde. Daraus wurde geschlussfolgert, dass die höheren und stärker konzentrierten Gehalte mineral-assoziierten C_{org} in den tonärmeren Böden in angehäuften Anordnungen festgesetzt sind. Die Anordnung von OBS in solch einer voluminösen Anordnung erklärt weshalb die Ansammlung von OBS von der Größe der Mineraloberfläche entkoppelt ist und daher keine Begrenzung für Potential der Ansammlung von C_{org} darstellt.

Die Wechselwirkungen zwischen unterschiedlichen Primärpartikeln im Boden und der Größenverteilung von Mikroaggregaten wurden in Studie III überprüft mittels der tonreicheren Böden des Tongehaltsgradienten bei 16–37 % auf der landwirtschaftlichen Forschungsstation in Scheyern. Eine neuartige Herangehensweise anhand von dynamischer Bildanalyse ermöglichte es, die Größenzusammensetzung aus Aggregaten, aggregierten Partikeln und unaggregierten Partikeln in nassgesiebten freien Größenfraktionen sowie nassgesiebten und ultraschallbehandelten okkludierten Größenfraktionen <250 μm zu unterscheiden. Dies gibt Auskunft über den präferentiellen Größenbereich von Mikroaggregaten, welcher bei etwa 30 μm festgestellt wurde, und das unabhängig vom Tongehalt. In den tonreicheren Böden wurden allerdings mehr Makroaggregate >250 und größere Mikroaggregate im Größenbereich 50–180 μm gefunden. Der Aufbau größerer Aggregate mag wiederum durch größere Anteile von Sandkörnern >100 μm in den tonärmeren Böden gehemmt sein. Die nassgesiebte Fraktion >250 μm enthielt lediglich 4 % mehr tongroße Partikel über den gesamten

Tongehaltsgradienten, was eine Voraussetzung für die Stabilisierung dieser größeren Makroaggregate sein könnte. Die kleine Größenfraktion <53 μm enthielt höhere C_{org} Konzentrationen als die Größenfraktion 53–250 μm, insbesondere in den Böden mit niedrigen Tongehalten. Trotz dieser Unterschiede der C_{org} Konzentrationen, unterscheidet sich die Zusammensetzung der OBS in den Fraktionen nicht zwischen den Tongehalten, aber zwischen den Größenfraktionen, wie durch die niedrigeren alkyl:O/N-alkyl Verhältnisse der Größenfraktion 53–250 μm mittels ^{13}C Kernspinresonanzspektroskopie angedeutet. Der Einfluss der Bodentextur stabilisiert vornehmlich größere und mehr Aggregate und trägt so auf indirektem Weg zur Ansammlung von OBS bei.

Unterschiedliche Zerfallsmechanismen der Bodenmikroaggregate, wie Dispersion oder Auseinanderbrechen, und deren Zusammenhang mit Bodeneigenschaften wurden in Studie IV in einem Vergleich verschiedener Gewinnungsmethoden untersucht. Dafür wurde eine neu entwickelte Vorgehensweise verwendet zur mechanischen Gewinnung von Mikroaggregaten durch uniaxiale Kompression aus den Böden der landwirtschaftlichen Forschungsstation in Scheyern. Im Vergleich mit nassgesiebten Proben, weisen die trockenseparierten Fraktionen eine höhere mechanische Stabilität und bakterielle Diversität auf. Dies war eng mit unterschiedlichen Zerfallsmechanismen und Größenzusammensetzungen der Partikel verknüpft, je nach Gewinnungsmethode. Trockenseparierte Mikroaggregate waren größer und enthielten mehr sandgroße Partikel, welche nach Befeuchtung dispergierten. Dies führte zu kleineren Mikroaggregaten, welche mehr feine Partikel enthielten als die trockenseparierten Mikroaggregate. Um den Einfluss unterschiedlicher Bodentexturen auf die Größe von Mikroaggregaten zu untersuchen, wurden Böden mit unterschiedlichen Tongehalten verglichen (19 %, 24 % and 34 %). Gemäß dynamischer Bildanalyse wiesen die trockenseparierten Mikroaggregate bis zu 40 μm höhere Durchmesser auf durch den höheren Anteil sandgroßer Partikel in den Aggregaten. Diese sandgroßen Partikel führten auch zu einer Verdünnung der C_{org} Gehalte in der trockenseparierten Größenfraktion 53–250 μm bei sinkenden Tongehalten. Aus der Auswirkung der Gewinnungsmethoden auf die Größe und Eigenschaften von Mikroaggregaten zeigt sich, dass die Trockenseparierung eine nützliche Alternative zur Nasssiebung darstellt, wenn Aggregate mit Einschlüssen sandgroßer Partikel erhalten werden sollen.

Insgesamt zeigen die Ergebnisse dieser Arbeit ausgeprägte räumliche Verteilungsmuster auf, die die Ansammlung von OBS in Bodenmikroaggregaten antreiben. Beide Studien I und II zeigen, dass sich die Ansammlung von OBS an bestimmten Stellen der Mineraloberfäche in den Fraktionen feiner Mineralpartikel ballt. Allerdings lässt sich aus der unvollständigen Bedeckung von Oberflächen und der dreidimensionalen Erweiterung des von OBS-bedeckten

Oberflächenanteils schließen, dass die Ansammlung organischer Substanz weitgehend von der Größe der Mineraloberflächen entkoppelt ist, an denen sich OBS zwar anfänglich sammeln kann aber anscheinend nicht durch die Verfügbarkeit von Mineraloberfläche behindert wird. Stattdessen stellt die angehäufte Anordnung von OBS ein unabhängiges Konzept dar für das Potential C_{org} in Böden zu speichern. Auf der Größenskala von Mikroaggregaten stabilisieren feine Mineralpartikel größere Aggregate in nassgesiebten Fraktionen sowie mehr okkludierte partikuläre OBS in den Böden mit höheren Tongehalten der Studien II und III. Aus dem Vergleich von Methoden zur Gewinnung von Mikroaggregaten in Studie IV ergibt sich, dass sandgroße Partikel einen Teil trockenseparierter Aggregate darstellen, aber nach Befeuchten dispergieren, was die Korrelationen mit den C_{org} Konzentrationen beeinflusst. Diese Ergebnisse zeigen wie die Bodentextur indirekt die Ansammlung von OBS durch Bildung von Aggregatarchitekturen fördert, die OBS stabilisieren, aber auch sandgroße Partikel. Die Ergebnisse dieser Arbeit weisen auf räumlich aufgelöste Wechselwirkungen hin, welche die Ansammlung von OBS auf der Mikroskala von Mineraloberflächen und Mikroaggregaten in Böden steuern.

III List of Studies

This work is based on the following four first-authored research studies. All studies are attached as appendices A–D.

Study I	
Title	Rapid soil formation after glacial retreat shaped by spatial patterns of organic matter accrual in microaggregates
Authors	S. A. Schweizer*, C. Hoeschen*, S. Schlüter, I. Kögel-Knabner and C. W. Mueller
Publication	Global Change Biology 24 (2018), 1637–1650. 10.1111/gcb.14014
Objectives	Develop a novel image analysis protocol to automatically quantify spatial segments of elemental distributions based on NanoSIMS measurements. Apply this method to investigate spatial patterns of heterogeneous microscale OM coverage in clay-sized soil fractions along a chronosequence in the forefield of the retreating Damma glacier (Switzerland). Relate the microspatial patterns with initial formation of soil structure and accrual of OM over the time after glacial retreat.
Results and conclusions	Over time after glacial retreat, successional spatial patterns of OM accrual were observed based on a machine-learning segmentation of $^{16}O^-$, $^{12}C^-$ and $^{12}C^{14}N^-$ distributions. The microspatial coverage of OM patches at mineral surfaces increased rapidly within several decades. Along the initial formation of soil structures, patchy-distributed OM developed into more connected structures. Despite the accrual of OM, the mineral surface was not completely masked which demonstrates that OM sequestration was decoupled from mineral surfaces. The CN:C ratio of OM patches reflected the development of relatively more N-rich compounds after several decades according to previous results from microbial and plant ecology.
Contributions	Leading of development and application of novel image analysis for NanoSIMS measurements, writing and revision of manuscript with input from co-authors

* Equal contribution

Study II	
Title	Piled-up organic matter decouples soil carbon sequestration from mineral surface area
Authors	S. A. Schweizer, C. W. Mueller, C. Hoeschen, P. Ivanov and I. Kögel-Knabner
Publication	Unpublished
Objectives	Analyze the control of fine mineral particles on OM sequestration. Determine the distribution of OM within particulate and differently sized mineral-associated density fractions using an arable topsoil with a clay content gradient. Derive measures for the amount of OM arranged and associated with mineral surface areas within fine mineral-associated fractions.
Results and conclusions	Throughout the clay content gradient, the soils contained similar concentrations of OM in the bulk soil. After density fractionation, a changing relationship of OM sequestration mechanisms was observed in soils with lower clay content compared

	to soils with higher clay content. Although the high-clay soils provide more mineral surface areas to potentially associate with OM, more OM is allocated to particulate OM occluded in aggregates. The OC concentrations of all fine mineral-associated fractions were higher in the low-clay soils and decreased to certain minimum values in the soils with higher clay contents. Despite high differences in the specific surface area of mineral-associated fractions <6.3 µm, the OC concentrations were similar. The specific surface area related to the mineral-associated OM in the fine silt-sized fraction and the coarse-clay sized fraction was constant throughout the clay content gradient. The image analysis of OM coverage based on NanoSIMS images reflected this finding. Accordingly, the amount of OM concentrated on this specific surface area was higher in the low-clay soils demonstrating that the OM is arranged in piled-up assemblages. Such voluminous arrangement provides quantitative evidence of the substantial amounts of OM that can be sequestered by decoupling OM sequestration from mineral surface area.
Contributions	Analysis of all data (partially based on previously unpublished results), additional surface area measurements and image analysis of NanoSIMS measurements, writing and revision of manuscript with input from co-authors

Study III	
Title	Soil microaggregate size composition and organic matter distribution as affected by clay content
Authors	S. A. Schweizer, F. B. Bucka, M. Graf-Rosenfellner and I. Kögel-Knabner
Publication	Geoderma 355 (2019), 113901. 10.1016/j.geoderma.2019.113901
Objectives	Quantify the effect of soil clay content on the mass proportions and size composition of free and occluded soil microaggregate-sized fractions. Differentiate the size composition of particles and aggregates within the size fractions and identify preferential size ranges of aggregates. Compare the concentration and composition of OM in size fractions across the clay content gradient. Relate the OM concentrations within the size fractions with their specific surface area.
Results and conclusions	Independent of clay content, most water-stable soil microaggregates <250 µm were found to be 30 µm in diameter. Soils with higher clay contents were found to contain more macroaggregates >250 µm and larger aggregate diameters in the 50–180 µm size range. In the soils with lower clay contents, higher sand grain contents could have impeded the buildup of larger aggregates. A difference of 4 % clay content were involved in stabilizing water-stable macroaggregates in contrast to microaggregates. Besides the smaller aggregate diameters, the size fractions from the soils with lower clay contents contained higher OM concentrations compared to the soils with higher clay contents. Most of the OM in low-clay soils is, therefore, held in small aggregate fractions. The OM composition indicated differences between the size fractions but not between clay contents. In the larger size fraction 53–250 µm, the alkyl:O/N-alkyl ratio was lower compared to the smaller size fractions <53 µm, according to ^{13}C nuclear magnetic resonance spectroscopy. It was concluded that soil texture controls the OM stabilization mostly indirectly, depending on the distribution of OM in different aggregate fractions.

Contributions	Analysis of all data, writing and revision of manuscript with input from co-authors

Study IV	
Title	Wet sieving versus dry crushing: Soil microaggregates reveal different physical structure, bacterial diversity and organic matter composition in a clay gradient
Authors	V. J M. N L. Felde*, S. A. Schweizer*, D. Biesgen, A. Ulbrich, D. Uteau, C. Knief, M. Graf-Rosenfellner, I. Kögel-Knabner and S. Peth
Publication	European Journal of Soil Science (2020), 1–19. 10.1111/ejss.13014
Objectives	Compare two different isolation protocols of microaggregate-sized fractions, wet sieving and dry crushing, based on mechanical stability, organic carbon contents and bacterial diversity. Differentiate aggregate failure mechanisms and how these explain the size distributions of the isolated size fractions. Investigate the effect of clay content on the aggregate and particle size distribution, organic carbon concentration, organic matter composition and the mechanical stability of dry-crushed microaggregate-sized fractions.
Results and conclusions	Dry crushing produced microaggregates <250 μm with a higher mechanical stability and bacterial diversity compared to wet-sieved samples. This was explained by different failure mechanisms activated depending on the mechanical impact of uniaxial crushing or the hydraulic pressure and dispersion in water. The influence of the isolation method greatly influenced the particle size composition of the fractions. The microaggregates isolated by dry crushing contained sand-sized primary particles, which led to aggregates of up to a 40 μm larger diameter. When submerged in water, these sandy microaggregates collapsed to 25 μm large structures when submerged in water. The inclusion of sand-sized primary particles in dry-crushed microaggregates was related with a dilution of OC concentrations in the size fraction 53–250 μm. Therefore, wet sieving might be a suitable isolation method to investigate OM dynamics, whereas dry crushing provides an advantageous alternative when microaggregates with sand-sized particles need to be preserved.
Contributions	Joint conceptualization of the study, measurement of size distributions and C and N concentrations, analysis of results in relation with other observations, writing of initial draft and active joint development of the manuscript with further data input from co-authors

* Equal contribution

Other studies with co-author contributions that are cited in this thesis include:

Krause et al. 2018	
Title	Microaggregate stability and storage of organic carbon is affected by clay content in arable Luvisols
Authors	L. Krause, A. Rodionov, S. A. Schweizer, N. Siebers, E. Lehndorff, E. Klumpp, W. Amelung
Publication	Soil and Tillage Research 182 (2018), 123–129. 10.1016/j.still.2018.05.003
Contributions	Measurement of soil texture and Fe and Al (oxyhydr)oxides contents, written contributions to the manuscript and active support of its revision

Krause et al. 2019	
Title	Initial microaggregate formation: Association of microorganisms to montmorillonite-goethite aggregates under wetting and drying cycles
Authors	L. Krause*, D. Biesgen*, A. Treder, S. A. Schweizer, E. Klumpp, C. Knief and N. Siebers
Publication	Geoderma 351 (2019), 250–260. 10.1016/j.geoderma.2019.05.001
Contributions	Joint development of image analytical methods for fluorescence images, analysis of results in relation with other observations, written contributions to the manuscript and active support of its revision

* Equal contribution

IV Table of contents

I Summary iii

II Zusammenfassung vi

III List of studies x

IV Table of contents xiv

1 Introduction 1

1.1 Soil microaggregates and the sequestration of organic matter 1

1.2 The role of fine mineral particles for soil organic matter dynamics 2

1.3 Advancing analytical approaches at the microscale 4

1.4 Soil aggregation related with soil texture 5

1.5 Dry and wet approaches to isolate soil aggregates 6

1.6 Objectives and approach 8

2 Material and Methods 10

2.1 Natural soil gradients 10

2.1.1 Damma glacier chronosequence (Study I) 10

2.1.2 Clay content gradient (Studies II–V) 11

2.2 Laboratory analytical methods 12

2.2.1 Soil texture analysis (Study V and adapted in Studies II–IV) 14

2.2.2 Clay mineral composition and Fe and Al (oxyhydr)oxides (Study II) 14

2.2.3 Density and size fractionation (Studies I and II) 15

2.2.4 Isolating microaggregate-sized fractions by wet sieving and dry crushing (Studies III and IV) 16

2.2.5 Analyses of organic matter in bulk soil and fractions (Studies I–IV) 17

2.2.6 Specific surface area as proxy for the microstructural arrangement of OM (Studies II and III) 17

2.2.7 Mechanical stability and bacterial community analysis (Study IV) 18

2.3 Microscale analyses 19

2.3.1 Preparation of soil samples and NanoSIMS analysis (Studies I and II) 19

2.3.2 Multichannel machine-learning segmentation and image analysis (Studies I and II) 20

2.3.3 Morphological analysis by optical microscopy and microtomography (Study IV) 23

2.3.4 Size distribution of wet-sieved and dry-crushed microaggregates (Studies III and IV) 23

2.4 Statistical analyses 26

3 Results and discussion 27

3.1 Initial soil formation related with successional establishment of OM patches at the microscale 27

3.2 Organic matter distribution and arrangement decoupled from clay content 29

3.3 Wet-sieved microaggregate diameters and occlusion of particulate organic matter mediated by clay content 32

3.4 Dry crushing isolates soil microaggregates influenced by soil texture 34

4 Conclusions and outlook 37

5 References 39

6 Acknowledgments 49

7 Appendix 51

A Study I 51

B Study II 52

C Study III 53

D Study IV 54

E Eidesstattliche Erklärung 55

F Curriculum Vitae summary 56

G List of scientific contributions 58

G.1 Peer-reviewed publications 58

G.2 Conference presentations (only first-authored) 58

G.3 Media contributions 60

1 Introduction

1.1 Soil microaggregates and the sequestration of organic matter

Soil structure is a fundamental property of soil that has long been of interest to scientists and land managers as it controls a broad range of soil processes (Atterberg, 1917; Edwards and Bremner, 1967; Wollny, 1898). The stability and arrangement of various soil constituents and pore spaces are critical for a soil's capacity to provide physical support for plants, resist soil erosion, receive, hold and transport water, cycle essential nutrients and aerate soils (Dexter, 1988; Kay, 1998). Earlier studies observed a deterministic pattern of aggregate failure with higher stability operating at smaller size scales (Edwards and Bremner, 1967; Field and Minasny, 1999; Oades and Waters, 1991; Raine and So, 1994). Derived from such breakdown patterns, microaggregates (<250 μm) were recognized as soil structural units built of composite building units (Miller and Jastrow, 1990; Tisdall and Oades, 1982). In turn, microaggregates are weakly associated to form macroaggregates at a higher hierarchical level (Christensen, 2001; Edwards and Bremner, 1967; Oades and Waters, 1991). This was also shown to be reflected in the dynamic buildup and decay rates of these structural units: Microaggregates turned over slower, were less susceptible to a changing soil environment and demonstrated a higher stability than macroaggregates (Jastrow et al., 1996; Lobe et al., 2011; Puget et al., 2000; Virto et al., 2008). Studies have shown that microaggregates can be formed while being occluded in macroaggregates (Angers et al., 1997; Oades, 1984; Six et al., 2002). The arrangement of particles within aggregates and their respective arrangement in even larger aggregates lead to an intricate arrangement of soil structure with physical disconnection of OM as a protective mechanism and the breakup of soil structure as a cause for the decomposition of OM (Chaplot and Cooper, 2015; Schmidt et al., 2011; Schrumpf et al., 2013; Segoli et al., 2013; Wiesmeier et al., 2019). While numerous studies have advanced a better understanding of the formation and breakdown mechanisms of macroaggregates and the responses of these large structural units to biological factors (e.g. Chaplot and Cooper, 2015; Golchin et al., 1994; Six et al., 2004; Tisdall, 1994), mechanistic insights into aggregate dynamics lack in-depth analyses of microaggregates and their diverse structural arrangement of soil components (Totsche et al., 2018). Due to their smaller size, microaggregates might be shaped and stabilized more specifically by fine reactive mineral soil components, microbial attachment and properties of OM components, in contrast to macroaggregates. As a result of this, microaggregate structures were shown to be more stable and have longer turnover times than macroaggregates, which highlights the importance of soil aggregate sizes for OC turnover and storage (Angers et al., 1997; Six et al., 2000; Trivedi et al.,

2017). Due to the pivotal role of soils in the terrestrial carbon cycle, further knowledge especially about the arrangement of OM in soil microaggregates is imperative to better understand the sequestration potential of organic carbon (OC) in soils facing unprecedented strain from global change (Kopittke et al., 2019; Smith et al., 2016).

1.2 The role of fine mineral particles for soil organic matter dynamics

The capability to globally harbor more OC than stored in the phytomass and the atmosphere (Lal, 2018; Scharlemann et al., 2014) make soils an important component of the global carbon cycle. In particular, the potential of agricultural soils for carbon sequestration is recently discussed to assess its contribution to efforts of climate change mitigation (Loisel et al., 2019; Mayer et al., 2018; Sanderman et al., 2017; Schlesinger and Amundson, 2019). The understanding of dynamic responses of soil OC leading to its emission as CO_2 or sequestration with a long-term potential has profound repercussions at the science-policy interface (Chabbi et al., 2017; Paustian et al., 2016; Sulman et al., 2018). In mineral soils, which are estimated to account for 79 % of the total soil OC stocks in the top 3 m (Scharlemann et al., 2014), various protection mechanisms related with fine mineral particles were postulated to drive OC sequestration (Rasmussen et al., 2018; Torn et al., 1997). More than half of the OC in arable soils were found within clay and silt-sized fractions according to many studies of the carbon distribution across different particle size fractions (Balesdent et al., 1988; Christensen, 1992; Gregorich et al., 1988). As a proxy for the content of fine mineral particles, the mass proportion of silt-sized and clay-sized particles has gained considerable importance in modelling efforts to predict a soil's 'capacity' to sequester OC (Hassink, 1997; Stewart et al., 2007) and is used to predict OM dynamics in modelling approaches (Bosatta and Ågren, 1997; Campbell and Paustian, 2015). These led to the notion that a soil with a higher proportion of fine mineral particles provides a higher potential to sequester OM. The mechanism underlying these empiric concepts rely on reactive mineral surfaces that dictate their association with OM. Such reactive mineral surfaces comprise mostly phyllosilicates and Fe/Al (oxyhydr)oxides with a high specific surface area (Churchman, 2018; Heckman et al., 2018; Rasmussen et al., 2018). Many studies derive their findings on the effect of fine mineral particle content on OM based on empiric relations from soil gradients at landscape scales or meta-studies across various climate variables (Amelung et al., 1998; Burke et al., 1989; Vaughan et al., 2019), soil horizons (Kaiser and Guggenberger, 2003; Souza et al., 2017) or parent material (Barré et al., 2017; Sollins et al., 2009; Vaughan et al., 2019), since these naturally do often correlate with themselves or the amount

of fine mineral particle. The role of land management was shown to decrease the steepness of the regression between the fine mineral particle content and the OC content of the soil (Feller and Beare, 1997; Feng et al., 2013). Making a model with so many covariates hampers the analysis of an isolated effect of fine mineral particles on OM dynamics. Instead of leading to increased association of OM at the mineral surface scale, increased proportions of fine mineral particles may also feed back into the stabilization of larger soil structures, which can occlude partly decomposed plant residue and inhibit their turnover (Schmidt et al., 2011; Virto et al., 2010). A constant ratio of silt-sized to clay-sized particles (approximately 1.5) has been postulated to build 'true' microaggregates within size fractions (Balabane and Plante, 2004). The interactive effect of OM and fine mineral particles on soil physical behavior including the stabilization of soil aggregates was determined to be strongest at a constant ratio (1:10) of their mass proportions in the bulk soil (Dexter et al., 2008). Accordingly, the so-called 'complexed' OM was found to stabilize fine mineral particles and lead to a lower dispersal of fine mineral particles (Dexter et al., 2008). The empirical relationship between bulk soil clay content or its dispersibility and the OM content was used in many studies as a proxy for soil structure stabilization (Barré et al., 2017; Graf-Rosenfellner et al., 2016; Jensen et al., 2019; Oades, 1988; Schjønning et al., 2012). An increasing content of fine mineral particles was mostly related with an increasing tensile strength of dry aggregates (Kay and Dexter, 1992). This might lead to a longer turnover of the OM in the aggregate, but could also limit the occlusion of litter-derived OM. The conceptual frameworks relating fine mineral particles with OM dynamics lack direct observations at the microscale that are needed to mechanistically understand whether more fine mineral particles lead to a stronger sorptive stabilization of OM or more stable microaggregate structures, which would both lead to an increased sequestration of OM in soil.

The reactivity of fine mineral particles varies depending on the soil mineral composition (Carroll, 1959; Macht et al., 2011), which is why many studies have found empiric relationships between mineral composition and OM dynamics (Barré et al., 2017, 2014; Feng et al., 2013; Kaiser and Guggenberger, 2000; Vogel et al., 2015; Wiseman and Püttmann, 2005). In contrast, many studies found no clear relationships between phyllosilicate mineral composition and OM content in particle fractions (Fernández-Ugalde et al., 2016; Pronk et al., 2013; Wattel-Koekkoek et al., 2001), whereas this can differ depending on the density (Sollins et al., 2009) and size (Fernández-Ugalde et al., 2013) of the isolated soil fraction. Such a high variability of results demonstrate that the concept of soil mineral reactivity dictating OM sequestration requires further mechanistic insights to explain the seemingly arbitrary relationship. A comparison of the fine clay-sized fraction (64 $m^2 g^{-1}$ specific surface area (SSA)) with the coarse clay-sized fraction (24 $m^2 g^{-1}$ SSA) has shown higher OM concentrations in the latter which

was related with a higher content of Fe (oxyhdr)oxides (Kahle et al., 2003). This shows that the reactivity of mineral surfaces towards OM can be limited to a specific part of the total SSA depending on the interplay with other mineral phases. A recent study advocated the composition of mineral-associated OM to be determined by a so-called 'mineral filter' compared with a 'microbial filter' related to the microbes that decompose plant and microbial-derived OM (Mikutta et al., 2019). Other studies concluded that there is an interplay of such two OM binding mechanisms according to density fractionation. Sollins et al. (2009) showed that OM in density fractions 1.8–2.6 g cm^{-3} is more derived by microbes, whereas the OM in the density fraction >2.6 g cm^{-3} is more influenced by the mineral surface composition. Wagai et al. (2018) showed that larger aggregates are controlled by OM input and its rapid decomposition, whereas smaller aggregates are more dependent on reactive Fe and Al (oxyhydr)oxides. All these studies show that the predominant composition of OM in the bulk soil can be governed by both minerals and microbial OM decomposers to different extents. At the microscale, such a co-existence implies that these mechanisms are spatially arranged alongside each other in an intact soil structure. For a better understanding on the driving factors underlying OM dynamics, it is therefore crucial to incorporate the spatial arrangement of OM into novel research approaches and relate it with potential interactions with mineral, microbial or molecular soil properties.

1.3 Advancing analytical approaches at the microscale

Based on earlier observations of N_2 sorption kinetics it has been postulated that OM is not distributed evenly as a monolayer across mineral surfaces and rather accumulates on a minor part of the total mineral surface (Kahle et al., 2002a, 2002b; Mayer, 1999). Developments of analytical techniques provided direct observations of mineral surfaces at the microscale with OM being distributed unevenly across mineral surfaces (Chenu and Plante, 2006; Ransom et al., 1997). The heterogeneous distribution of soil reactive minerals and surface properties might be partially responsible for the arrangement of OM in discrete patches instead of homogeneous coatings (Kleber et al., 2015). An experiment with the incubation of isotope-labelled litter in a soil has shown that fresh OM is preferentially retained at already existing mineral-associated OM surfaces (Vogel et al., 2014). This might be related with the spatial distribution of microbial colonies and favorable surface conditions of OM patches (Kleber et al., 2015). For a better understanding of OM sequestration processes, correlated approaches of traditional bulk soil analyses need to be combined with targeted applications of microscale techniques capturing the heterogeneity of intact soil structures. Novel applications of spectromicroscopic techniques

provide insightful tools at the microscale and submicroscale (Rennert et al., 2012). Among them, nanoscale secondary ion mass spectrometry (NanoSIMS) enabled powerful measurements of the spatial distribution of various ion species at a lateral resolution of approximately 100 nm (Hatton et al., 2012; Herrmann et al., 2007; Mueller et al., 2013; Remusat et al., 2012). Despite widespread approaches to visualize the heterogeneous distribution of OM, there is only little information on the systematics that drive the spatial arrangement of OM at the microscale. Advanced analytical efforts are needed to derive deterministic spatial patterns from spectromicroscopic observations that govern the heterogeneous distributions of soil constituents.

1.4 Soil aggregation related with soil texture

The arrangement of soil constituents of various sizes into a larger architecture can impose a heterogeneous distribution of reactive mineral surfaces, their accessibility and other microenvironmental soil properties, like pore connectivity, water and air availability or OM distribution. Earlier observations on the influence of the distribution of OM within the mineral matrix of a soil on OM properties were inferred by the distinct chemical compositions of density fractions (Golchin et al., 1994) and the natural ^{13}C abundance in size fractions (Six et al., 1998). An analysis of spatial patterns of elemental distributions within a thin section of a macroaggregate, showed mainly two recurring types of microarchitectures including coarse Si-rich mineral particles compared with fine mineral particles densely occluding particulate OM (Steffens et al., 2017). In contrast to a random distribution of mineral particles, the functionality of microaggregates is determined, therefore, by defined mineral assemblages shaping the aggregate architecture. Most studies on soil aggregates rely on techniques to isolate these stable soil structural entities using wet sieving and sonication. The water immersion during wet sieving leads the slaking and dispersion of soil structures according to differential swelling and air entrapment (Le Bissonnais, 1996). Such destabilization of aggregate structures reflects the influence of hydraulic and mechanical stress during wetting and drying. The additional mechanical impact from imploding vapor bubbles during sonication provides a quantifiable technique for the isolation of soil aggregates (Graf-Rosenfellner et al., 2018; Kaiser and Berhe, 2014). Clay content was mostly related with an increased stabilization of aggregates by using these isolation techniques (Amézketa, 1999). In turn, the volume occupied by coarse mineral particles like sand grains dilutes the soil structure and impedes the arrangement of other soil constituents. Therefore, most previous studies analyzing the relationship of OM on aggregate dynamics used a simple subtraction of the mass proportion of primary particles coarser than

the wet-sieved size fraction (Elliott et al., 1991; Kemper and Chepil, 1965; Six et al., 2002), since most OC was found to be related with fine mineral soil particles. If the distribution and arrangement of all mineral soil particles within aggregates is of interest, the soil particles participating in aggregation have to be differentiated from free non-aggregated primary particles isolated in size fractions. Most studies focused on fine primary particles instead of larger sand-sized primary particles, since they did not play a major role for the sequestration of OM in aggregates. Through water menisci forces under changing water conditions, sand grains may draw fine mineral particles towards them and form stable aggregate structures (Ghezzehei and Or, 2000; Paradiś et al., 2017). The differentiation which of the particles in isolated size fractions participate in aggregation enables determining distinct types of aggregate structures, according to the proportion of aggregates in a size fraction, how many particles build these aggregates and how large the aggregate diameters are. Many previous studies have used density separation to differentiate presumably non-aggregated and heavier primary particles from lighter aggregates (Balabane and Plante, 2004; Moni et al., 2012; Virto et al., 2010, 2008). Such approach assumes that the lighter aggregate fraction is characterized by organo-mineral associations. To differentiate aggregation independent of density, dynamic image analysis (Kayser et al., 2019) can provide size distributions of size fractions which can be subjected to various treatments and induce a dispersion of the aggregates within the suspension. This provides detailed size distributions at a resolution of several μm of the whole size spectrum of microaggregates. The arrangement of soil particles within microaggregates can reveal the building patterns of these architectures.

1.5 Dry and wet approaches to isolate soil aggregates

In agricultural soils, the mechanical forces exerted during land management operations causes shear failure of the soil structure (Horn and Peth, 2012). Mechanical stress during field traffic or tillage operations can establish and reactivate pre-conditioned failures zones within soil aggregates (Horn and Peth, 2012). In a similar manner to such aggregate breakdown processes in arable soils, mechanical impact can be used for the dry separation of soil aggregates (Dexter and Kroesbergen, 1985; Obalum et al., 2019; Skidmore and Powers, 1982). The dry sieving in sieve shakers is often used to differentiate size fractions which are important microbial microhabitats (Bach and Hofmockel, 2014; Blaud et al., 2017). To isolate small-sized microaggregates, uniaxial crushing enables to break down dry soil aggregates along zones of mechanical weakness (Kristiansen et al., 2006). The fragmentation of soil structure by dry crushing might address different failure zones than the widely used wet sieving approaches.

Different failure zones would result in different size structures and properties of the isolated size fractions, whereas there is only little information comparing dry-separated fractions with wet-sieved ones. Differences in the aggregate and particle size distributions are expected to affect microbial activity and diversity, since the pore distribution and the accessibility of OM sources are affected (Bimüller et al., 2016; Ebrahimi and Or, 2018). Further information about the influence of the isolation methods like wet sieving and dry crushing is critical to relate size and structure properties of microaggregates in fractions with soil functions like OM sequestration and microbial habitat.

1.6 Objectives and approach

The analyses of soil microaggregate properties are at the center of this work according to structural properties (mass proportions of size fractions; aggregate and particle size distributions) and stability indices (dispersion during wet sieving and sonication; mechanical stability). The overall objective of this work is to better understand the relationships between soil microaggregates, the distribution of fine particles and the arrangement of OM at the microscale. To unravel the temporal dynamics of evolving organo-mineral associations and the influence of soil texture, soil gradients with differences in the time of soil formation and clay content were sampled and investigated using various fractionation procedures and analytical techniques at different spatial scales.

The four main objectives of this work are as follows;

Objective 1. *Spatial patterns of mineral-associated OM during the initial formation of microaggregates (Study I)*—Determine driving factors underlying the formation of organo-mineral associations in a newly developed soil, which sequesters OC in soil microaggregates for the long-term. Relate the accrual of OC in the bulk soil with the distribution of OM across mineral surfaces in clay-sized fractions. Quantify spatial patterns of the OM coverage, the connectivity of OM patches, as well as the C and N composition of OM patches at the microscale and determine their development over decadal and centennial timescales of soil formation.

The initial formation of microaggregates through association of OM with mineral surfaces was investigated with a chronosequence using an established 'space-for-time' substitution in the forefield of the Damma glacier. Microspatial patterns of OM dynamics were analyzed based on NanoSIMS measurements of elemental distributions and quantified using a newly developed image analysis protocol.

Objective 2. *Influence of clay content on OM distribution and arrangement (Study II)*—Investigate how differences in soil texture affect OC concentration and contributions of particulate and mineral-associated forms. Determine whether an increasing clay content leads to an increasing distribution of OC in clay and silt-sized fractions or a change of the OM composition. Visualize and quantify the mineral surface area which is associated with OM and understand how these are related across the clay content gradient.

To investigate the impact of fine soil particles on OM, topsoils samples from an agricultural research site with similar management and a wide range of clay content (5–37 % clay content) were taken. Density fractionation was used to determine the distribution of OM in particulate

and mineral-associated fractions. The arrangement of OM in fine mineral-associated fractions was analyzed by N_2-sorption and NanoSIMS measurements.

Objective 3. *Soil microaggregate size compositions and OM distribution as affected by clay content (Study III)*—Determine the effect of soil texture on free wet-sieved and occluded wet-sieved fractions. Differentiate aggregate size distributions from underlying particles to identify preferential sizes of microaggregates. Analyze the effect of different particle size compositions on OM concentration, contribution and chemical composition of size fractions.

Microaggregate-sized fractions were isolated from a clay content gradient (16–37 % clay) using wet sieving and dry crushing. In these size fractions, the size distributions of aggregates and particles were determined by dynamic image analysis. Differences in the structural arrangement of microaggregates across clay content were related with the distribution of OM and various other soil properties.

Objective 4. *Size composition and OM distribution in dry-crushed microaggregates as influenced by soil texture and their comparison with wet-sieved aggregates (Studies III and IV)*—Analyze size distributions of microaggregate-sized fractions isolated by dry crushing. Determine the effect of wetting and dispersion on the size distributions of aggregates and particles in dry-crushed fractions. Compare dry-crushed fractions with wet-sieved ones based on the size distributions, mechanical stability, OC concentration and bacterial community.

The size distributions of fractions isolated by uniaxial dry crushing were measured by dynamic image analysis in a dry state. To determine the dispersion of aggregates in a wet state, the size distributions of dry-crushed fractions were also measured after wetting and $Na_4P_2O_7$ dispersion. The size distributions were related with further properties, like their mechanical stability of selected microaggregates in a loading frame, the OM distributions across size fractions and the bacterial community composition and diversity.

2 Material and methods

2.1 Natural soil gradients

2.1.1 Damma glacier chronosequence (Study I)

To analyze the initial formation of soil structures at the microscale, soil samples originating from a chronosequence study in the forefield of the Damma glacier (Switzerland) (Fig. 1) were used (Dümig et al., 2012). In the proglacial environment, the mean annual temperature is 2.2 °C with a mean annual precipitation of approximately 2,400 mm, mostly snowfall (Dümig et al., 2012). The granite of the Aare Massif, deposited by the glacier, developed into initial soil stages after the retreat of the glacier. Based on a larger dataset across the centennial soil development, four stages were selected from the work of Dümig et al. (2011) (Fig. 1). The age of the development stages was determined based on movement records or aligned with movement records from neighboring glaciers (Bernasconi et al., 2011).

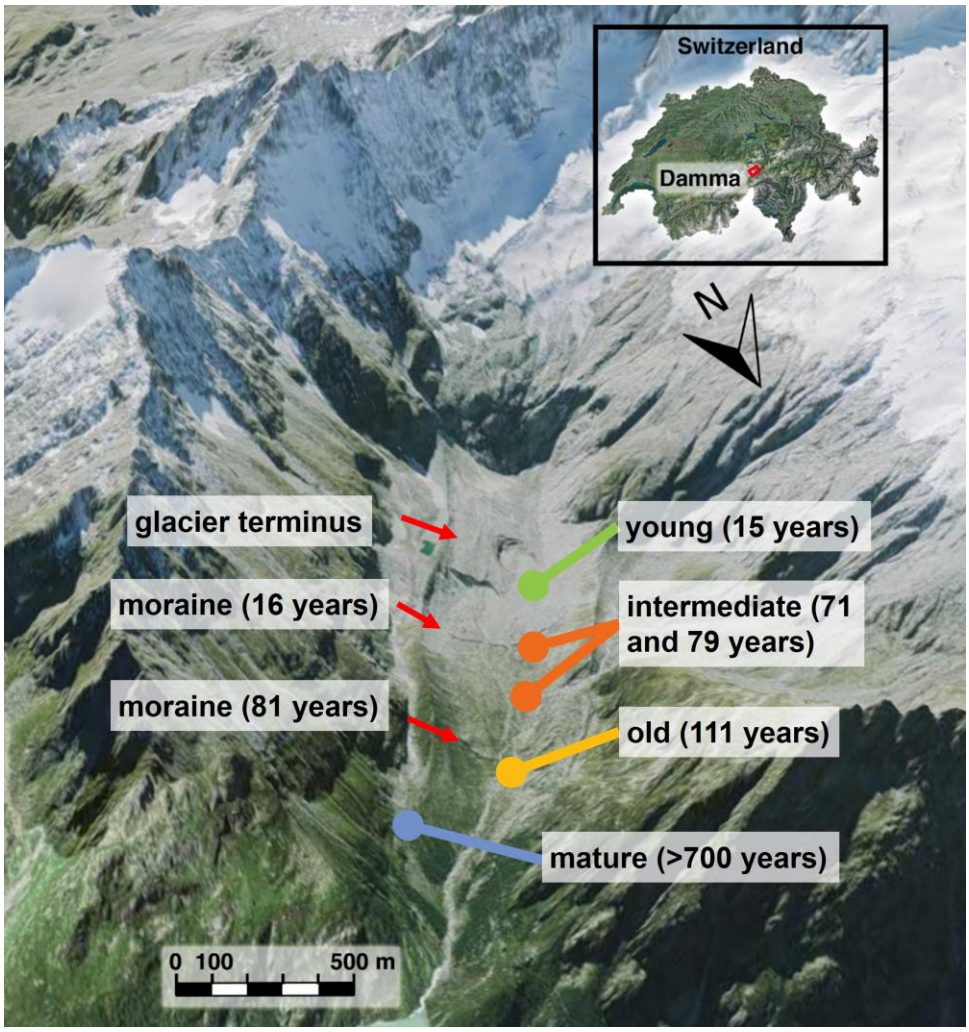

Fig. 1: Overview on the chronosequence by Dümig et al (2012, 2011) used to analyze initial soil formation and OC sequestration at mineral surfaces in Study I (modified based on Bundesamt für Landestopografie swisstopo).

2.1.2 Clay content gradient (Studies II–V)

To analyze the impact of varying fine soil particle contents on OM distribution, an agricultural research site with comparable land use management and parent material in Scheyern, 40 km north of Munich (Germany) (Fig. 2) was sampled as described by Kölbl and Kögel-Knabner (2004) and Krause et al (2018). The climate at the sampled research farm is characterized by a mean annual temperature of 7.4 °C and an average annual precipitation of 803 mm at 445–498 m above sea level. The large clay content gradient at the site has developed from different mixture ratios of Miocene Upper Freshwater Molasse which is heterogeneously covered by Quaternary loess. According to the World Reference Base for soil resources (FAO, 2014), the soils at the research site have been classified as Cambisols.

The agricultural research site has a long-standing history of intensive agricultural usage (Schröder et al., 2002). Following 1992, the land was managed using a harrow and a chisel plow instead of a moldboard plow. The sites were fertilized with synthetic N and cattle manure. According to a previous remote sensing studies (Sommer et al., 2003), the C input from wheat harvest residues was approximately 10 % higher when comparing the soils with 20 and 30 % clay content (Study III, 2.1). Although differing management practices in the two plots were implemented for some years after 1992, a comparison of samples from both plots at similar clay contents showed comparable distributions of OC.

Samples were taken in the top 0–20 cm of the soils, whereas the top 5 cm were discarded in case a dense crust had formed. The field fresh samples were passed through an 8 mm sieve and stored at 4 °C until further analysis.

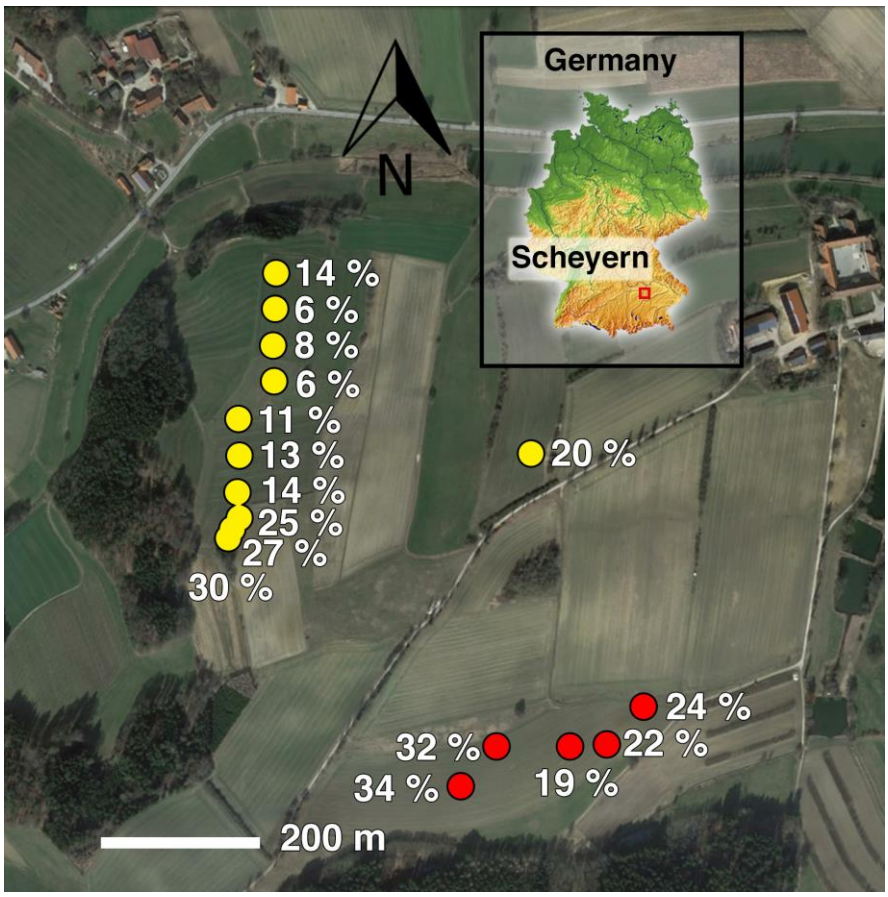

Fig. 2: Overview on sampling for Study II (yellow and red) and Studies III and IV (red). All sampled sites underwent a long history of arable farming within the same agricultural research site.

2.2 Laboratory analytical methods

The soil samples taken from the field were fractionated and analyzed according to various methods (Table 1) as detailed in the following chapters.

Table 1: Overview on (a) fractionation and (b) analytical methods in the Studies I–IV.

(a)

Method	Obtained fractions	Study
Combined density (1.8 g cm^{-3}) and size fractionation	Particulate† and mineral-associated OM fractions	II
Density fractionation (1.6 g cm^{-3})	Light and heavy mineral-associated OM fractions	I
Wet sieving and sonication	Free and occluded fractions in the size range of microaggregates	III
Dry crushing by uniaxial compression in loading frame	Dry-crushed fractions in the size range of microaggregates§	IV

(b)

Investigated property	Method	Study	Sample type
Soil texture	H_2O_2 oxidation, wet sieving, X-ray attenuation	V (II–IV)	Bulk soil
Clay mineral composition	X-ray powder diffraction‡	II	Clay fractions (<2 μm)
Fe and Al (oxyhydr)oxides	Ammonium oxalate and dithionite-citrate-bicarbonate extracts measured by ICP-OES	II	Bulk soil
OC and N concentrations	Dry combustion by CN analyzer	I	Clay-sized fractions (<2 μm)
		II	Particulate and mineral-associated OM fractions
		III	Wet-sieved size fractions <250 μm
		IV	Dry-crushed size fractions <250 μm
		V	Bulk soil
Radiocarbon signature $\Delta^{14}C$	AMS$	II	Mineral-associated fine fractions
OC composition	^{13}C NMR spectroscopy	II	Mineral-associated fine fractions
		III	Wet-sieved size fractions <250 μm
		IV	Dry-crushed size fractions <250 μm
Specific surface area and piling of OM	N_2-BET before and after NaOCl treatment	II	Mineral-associated fine fractions
		III	Wet-sieved size fractions <250 μm
Size distributions	Dynamic image analysis	III	Wet-sieved size fractions <250 μm
		IV	Dry-crushed size fractions <250 μm
Elemental distributions and spatial patterns at microscale	NanoSIMS, ImageJ image analyses, preparative scanning electron microscopy	I	Clay-sized fractions (<2 μm)
		II	Coarse clay-sized (0.2–2 μm) and fine silt-sized fraction (2–6.3 μm)
Morphology at microscale	Microtomography§ and optical microscopy	IV	Dry-crushed size fractions <250 μm
Mechanical stability	Uniaxial compression with loading frame§	IV	Dry-crushed and wet-sieved size fractions <250 μm
Bacterial community composition and diversity	Amplicon sequencing of the 16S ribosomal RNA gene¶	IV	Dry-crushed and wet-sieved size fractions <250 μm

†Data partially adapted from Kölbl and Kögel-Knabner (2004), §Analyzed by V.J.M.N.L. Felde (Kassel), ‡Analyzed by P. Ivanov and K. Eusterhues (Jena), $Analyzed by Beta Analytic Inc., ¶Analyzed by D. Biesgen and C. Knief (Bonn)

2.2.1 Soil texture analysis (Study V and adapted in Studies II–IV)

The wide clay content gradient of 5–37 % clay content was determined through sieving and X-ray attenuation after H_2O_2 treatment by Krause et al. (2018) and Kölbl and Kögel-Knabner (2004). To remove OM, the samples were submerged with an excess of 30 % H_2O_2 until no further reaction could be observed. After sieving with a 2 mm and a 63 µm sieve, the size distribution of the <63 µm particles was determined through X-ray attenuation using a Sedigraph (Micromeritics).

2.2.2 Clay mineral composition and Fe and Al (oxyhydr)oxides (Study II)

Within Study II, the mineralogical composition of clay-sized fractions <2 µm was determined across a gradient of 16–37 % clay content using X-ray powder diffraction by P. Ivanov and K. Eusterhues at the Friedrich-Schiller-University Jena (Germany). After saturation of the samples with K^+ and Mg^+, the X-ray diffraction patterns of clay-sized fractions were analyzed at 3–32 ° 2Theta using a D8 Advance (Bruker). After the measurement, the Mg-treated samples were saturated with ethylene glycol whereas the K-treated samples were heated to 400 °C and 550 °C. Based on the characteristic responses of the diffraction patterns to the treatments, semi-quantitative contents of relative clay minerals were estimated (Biscaye, 1965). The clay mineral composition was dominated by Illite with low kaolinite and chlorite contents in all samples (Study II, Supp. Table 1). Low to moderate differences of smectite and vermiculite were found between samples. Minor concentrations of K- and Na-feldspars were also found.

For samples from across a gradient of 5–37 % clay content, Fe and Al (oxyhydr)oxide contents were determined using chemical extractions with acid ammonium oxalate (oxalate) and dithionite-citrate-bicarbonate (DCB). The oxalate extraction is assumed to target non-crystalline phases, whereas the DCB extraction was sequentially used to estimate remaining crystalline Fe and Al oxides. The oxalate extraction was performed according to Schwertmann (1964) including 2 h shaking of the samples in the dark. The supernatant of the samples was extracted after centrifugation (20, 000 g for 20 min) and filtration (0.2 µm, regenerated cellulose, Phenomenex®). After two washing steps of the residual soil sample with water, the second extraction with DCB was achieved following Mehra and Jackson (1958). The samples were shaken for 16 h and the supernatant extracted as described previously. The Fe and Al

concentrations of the supernatants were determined using inductively coupled plasma optical emission spectroscopy of a Vista-Pro (Varian).

Across the gradient of 5–37 % clay content, the silt content and Fe and Al (oxyhydr)oxides increased linearly with clay content, whereas the sand content decreased. The clay content is, therefore, used as a proxy for fine and reactive mineral particles in this thesis, as also proposed by Churchman (2010).

2.2.3 Density and size fractionation (Studies I and II)

Combined density and size fractionation (Fig. 3) were used in both Studies I and II to fractionate two major forms of soil OM: partly decomposed and particulate plant residues and OM associated with mineral particles (Lavallee et al., 2019). In Study II, the floating free particulate OM was isolated after submerging the soil in sodium polytungstate solution of 1.8 g cm^{-3} and the occluded particulate OM was obtained after additional sonication at 450 J ml^{-1} according to Kölbl and Kögel-Knabner (2004). The mineral-associated fraction >1.8 g cm^{-3} was sieved to obtain size fractions 200–2000 µm, 20–200 µm and <20 µm. The fine fractions 6.3–20 µm, 2–6.3 µm and <2 µm were isolated from the <20 µm fraction using sedimentation. The clay-sized fractions <0.2 µm and 0.2–2 µm were isolated from the <2 µm fraction using centrifugation. To remove any remnants of the sodium polytungstate solution, all fractions were washed <1 µS cm^{-1} by pressure filtration (0.45 µm; cellulose nitrate) using deionized H_2O. Afterwards the fractions were freeze-dried for further analyses.

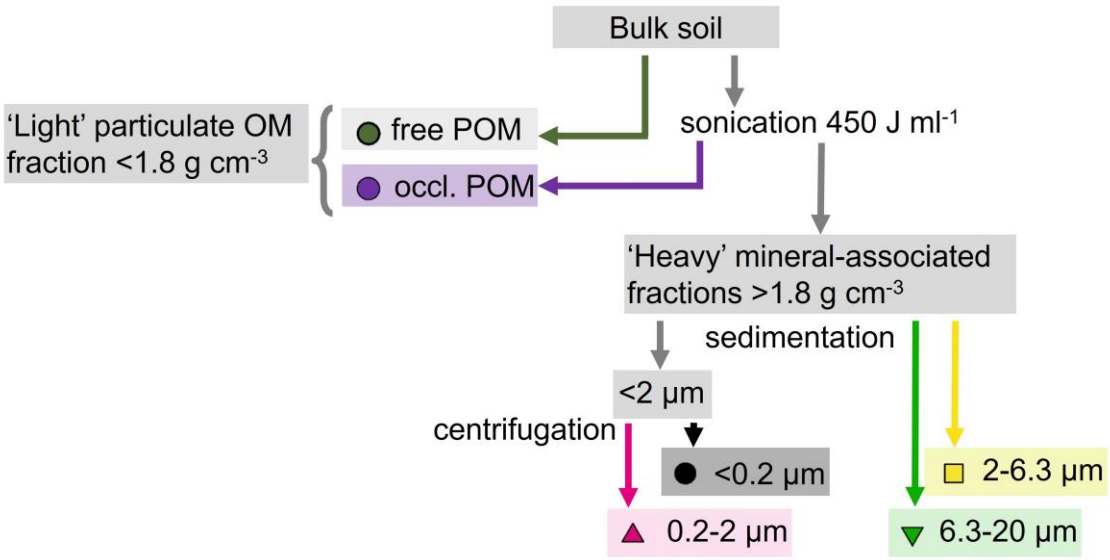

Fig. 3: Overview on the fractionation schema applied in Study II. The combined use of density and size fractionation techniques enabled the isolation of particulate OM fractions and mineral-associated OM fractions of different sizes.

For Study I on the soil development in the Damma glacier forefield, the mineral-associated fine fraction was isolated through submersion in sodium polytungstate solution >1.6 g cm^{-3} and dispersed with 200 J ml^{-1} (Branson Sonifier 250) by Dümig et al. (2012). After dispersion, the clay-sized fraction <2 μm was extracted as described previously by sedimentation, pressure filtration and freeze-drying. These previously isolated fractions were subjected to another density fractionation to differentiate newly formed organo-mineral associations from freshly weathered mineral particles for Study I. The clay-sized fraction >1.6 g cm^{-3} was separated into a light fraction (1.6–2.2 g cm^{-3}) and a heavy fraction (>2.2 g cm^{-3}) by density fractionation with sodium polytungstate. These fractions were obtained as described above.

2.2.4 Isolating microaggregate-sized fractions by wet sieving and dry crushing (Studies III and IV)

To isolate microaggregates, the soil samples were dispersed or fragmented into fractions in the size range of microaggregates using wet sieving and dry crushing. The soil fractions were obtained from the clay content gradient (16–37 %) by wet sieving for Studies III and IV and by dry crushing for Study IV. After a slow pre-wetting of field-fresh soil (<8 mm) for 30 min, the samples were submerged for wet sieving. A 250-μm sieve and a 53-μm sieve were manually oscillated for 5 min below the water. The free water-stable fractions <53 μm and 53–250 μm were freeze-dried for further analyses. To break down macroaggregates into microaggregates that were occluded in the macroaggregates, the water-stable fraction >250 μm was sonicated at 60 J ml^{-1} (Amelung and Zech, 1999) with a Branson Sonifier 250. After another wet sieving as described previously, the occluded size fractions <53 μm, 53–250 μm and >250 μm were recovered by freeze-drying. An additional 20-μm sieve was used to obtain additional free and occluded size fractions <20 μm in Study IV. The fraction >2 mm in the >250 μm fraction was weighed and subtracted from the initial sample weight.

Dry crushing was used to isolate microaggregate-sized fractions with a potentially different breakdown mechanism in Study IV. Dry-crushed fractions <250 μm were obtained from air-dried soil (<2 mm) by V.J.M.N.L. Felde at the University of Kassel (Germany) using a mechanical Allround Line loading frame (Zwick Roell). The sample was dry-crushed with uniaxial compression by slowly reducing the distance between the sample table and a piston to 250 μm. The disruption through mechanical loading assumes soil aggregates to break down according to potential failure zones within the structures. Depending on the stability, the number and the location of these failure zones, the soil structures may break into microaggregates of different sizes. The dry-crushed sample <250 μm was separated into the

size fractions <20 μm, 20–53 μm and 53–250 μm by tap sieving with a modified Casagrande apparatus at constant air humidity. To avoid the crushing of sand-sized primary particles >250 μm, the crushing speed was adjusted to a slow speed. The load-displacement curves of the piston (Study IV, Supp. Fig. 1) did not exhibit a distinct sharp peak which would indicate a sand grain rupture.

2.2.5 Analyses of organic matter in bulk soil and fractions (Studies I–IV)

To determine the distribution of OM in the soil, the concentrations of OC and total nitrogen were analyzed in bulk soils, density fractions and size fractions by dry combustion in a CN elemental analyzer (Vario EL, Elementar). In all studies, the soil samples were free of carbonates and contained no evidence of lime applications. To compare OC stocks in the top 0–20 cm across the wide gradient of 5–37 % clay content in Study II, calculations included the OC concentrations and the bulk density of fine earth <2 mm (stone content >2 mm excluded).

As a proxy for the turnover of OM, eight representative coarse clay-sized samples from the 5–37 % clay content gradient in Study II were used to determine the radiocarbon content using accelerator mass spectrometry by Beta Analytic Inc. (USA). The radiocarbon signature $\Delta^{14}C$ was computed as relative difference of the ^{14}C:^{12}C ratio compared to that of oxalic acid standard decay rate while correcting for the fractionation of radiocarbon according to $\delta^{13}C$ and sampling time.

To determine the chemical composition of OM, solid-state ^{13}C NMR spectroscopy was used in Studies II–IV. The samples were introduced into a DSX 200 NMR spectrometer (Bruker) using a spinning frequency of 6800 Hz while measuring at a resonance frequency of 50.3 MHz with cross-polarization magic angle spinning technique and a pulse delay of 0.4 s. The ^{13}C spectra was divided into major chemical shift regions by integration (alkyl C at 0–45 ppm; O/N-alkyl C at 45–110 ppm, aryl C at 110–160 ppm and carboxyl C at 160–220 ppm) also including spinning side bands (Knicker et al., 2005).

2.2.6 Specific surface area as proxy for the microstructural arrangement of OM (Studies II and III)

The specific surface area (SSA) provides an important index for reactive mineral surface area. The SSA of fine mineral fractions <6.3 μm from Study II and microaggregate-sized fractions from Study III were determined by N_2 sorption at 77 K using an Autosorb-1 analyzer (Quantachrome) based on the Brunauer-Emmett-Teller principle (Brunauer et al., 1938). To

remove any other adsorbate from the mineral surfaces, the samples were outgassed for 12 h under vacuum and constant helium flow at 40 °C.

For OM surfaces, the N_2 sorption technique is known to provide a SSA as low as 1 m^2 (g OM)$^{-1}$, which is much lower compared with mineral surfaces (Mayer and Xing, 2001; Theng et al., 1999). This property was used in Study II to measure the SSA related with OM association by determining the SSA difference before and after removal of OM. The OM was removed by treating the samples four times for 24 h with 1 M NaOCl at pH 8. The average degree of OC removal in Study II was 85 % (± 1 standard error) throughout the clay content gradient, corroborating previously reported degrees of OC removal (Feller et al., 1992; Mikutta et al., 2005). Afterwards, the treated fractions were washed with deionized H_2O until <50 µS cm^{-1} and obtained by freeze-drying for another SSA measurement. The difference of the SSA before and after OM removal provided a measure of how much OM is arranged and eventually piled on the mineral surface.

To get further insights about the arrangement of OM at mineral surfaces, the results of the OM piling index were related with monolayer-equivalent OC loadings according to complex proteins like insulin or albumin (Keil et al., 1994; Mayer, 1994). Proteinaceous macromolecules are used as model compounds of mineral-associated OM in several studies (Kleber et al., 2007; Moon et al., 2019). Based on positive linear correlations between SSA and OC concentrations, monolayer-equivalents of 0.5–1 mg OC m^{-2} were found for marine sediments and mineral soil (Keil et al., 1994; Mayer, 1994). To conceive the voluminous extension of mineral-associated OM, we estimated potential thicknesses based on measurements of the 3–5 nm extension of adsorbed α-synuclein and albumin (Ouberai et al., 2014).

2.2.7 Mechanical stability and bacterial community analysis (Study IV)

To measure the tensile strength of soil microaggregates, the same loading frame was used as for the isolation through dry crushing (Allround Line, Zwick Roell) by V.J.M.N.L. Felde at the University of Kassel (Germany). A high-resolution load cell enabled recording load-displacement curves and the total force of crushing 50 individual microaggregates, that were selected from each of the dry-crushed and wet-sieved size fraction 53–250 µm.

The bacterial community in the dry-crushed size fractions was analyzed by D. Biesgen and C. Knief at the University of Bonn (Germany). After DNA extraction from the dry-crushed and wet-sieved size fractions 20–53 µm and 53–250 µm, the 16S ribosomal RNA gene was amplified with polymerase chain reaction, sequenced and analyzed according to Maarastawi et

al. (2018). The operational taxonomic units were compiled from the sequencing data and the bacterial alpha-diversity and beta-diversity computed (Maarastawi et al., 2018).

2.3 Microscale analyses

2.3.1 Preparation of soil samples and NanoSIMS analysis (Studies I and II)

Several preparative steps were needed for the analyses of the microspatial arrangement of OM and mineral surfaces in fine silt-sized and clay-sized fractions in Studies I and II. Fine mineral-associated soil fractions <6.3 μm were applied onto Si wafer using 1–2 mg (10 ml $H_2O)^{-1}$. After drying the wafer in a desiccator at room temperature, the wafers were coated with approximately 5 nm Au under Ar atmosphere prior to scanning electron microscopy analyses and approximately 30 nm Au/Pd prior to NanoSIMS analyses in order to avoid charging. The wafers were examined by scanning electron microscopy to determine regions of interest with representative areas at the microscale containing particles and microaggregates. On each sample, numerous regions of interest were analyzed with NanoSIMS 50L (Cameca, Gennevilliers, France). A Cs^+ primary ion beam with 16 keV primary ion impact energy was used to implant reactive Cs^+ ions into the sample until a steady state of secondary ion yields is reached and collected at electron multipliers with a dead time of 44 ns. Thanks to the high mass resolution of the NanoSIMS, interference of the desired secondary ions with ions or cluster ions with a similar mass can be avoided. Before measurement, the regions of interest were pre-sputtered with a high energy using the Cs^+ beam to remove the Au/Pd coating. During the measurements secondary ion distributions were recorded for $^{12}C^-$, $^{16}O^-$, $^{12}C^{14}N^-$, $^{30}Si^-$, $^{32}S^-$, $^{27}Al^{16}O^-$ and $^{56}Fe^{16}O^-$ for Study I and for $^{12}C^-$, $^{16}O^-$, $^{12}C_2^-$, $^{12}C^{14}N^-$, $^{31}P^-$, $^{32}S^-$, $^{27}Al^{16}O^-$ and $^{56}Fe^{16}O^-$ for Study II. In Study I, different field of views were used depending on the size of particles like 30x30 m^2 with pixel dimensions of 256x256 pixels and a dwell time of 30 ms $pixel^{-1}$ or 40x40 μm with 512x512 pixels and 10 ms $pixel^{-1}$ dwell time and a primary ion current of 1 pA. In Study II, 40 planes of a field of view of 30x30 μm and 256x256 pixels were recorded with a dwell time of 1 ms $pixel^{-1}$ and a primary ion current of 2 pA. To compensate for charging effects on less conductive mineral surfaces, the internal electron flood gun in the NanoSIMS instrument was used.

2.3.2 Multichannel machine-learning segmentation and image analysis (Studies I and II)

A newly developed image analysis enabled the quantification of spatial patterns based on the measurements of elemental distributions. At the beginning, the NanoSIMS measurements were corrected for the dead time of the electron multiplier using OpenMIMS plugin for ImageJ (Gormanns et al., 2012). A segmentation mask was derived from the measurements using $^{16}O^-$ (indicative of mineral surfaces) and $^{12}C_2^-/^{12}C^-$ as well as $^{12}C^{14}N^-$ (indicative of organic matter) (Fig. 4a, b). The distributions of these three ion distributions were prepared for segmentation through a contrast enhancement of 0.5 % of the pixels (Schindelin et al., 2015). For the segmentation a machine learning algorithm implemented in Ilastik 1.2 (Sommer et al., 2011) was used. This approach enabled to simultaneously use multiple image features as input features like the intensity, gradient and edge detection of all three ion distributions at various spatial scales (Fig. 4c_1, c_2). Training areas, which covered <1 % of the total image area, were identified manually using maps of the relative uncertainty and supplied to the machine learning algorithm (Fig. 4c_3). The supervised classification was trained until areas of the relative uncertainty were confined to the borders of segments. All measurements were simultaneously processed into segmentation masks (Fig. 4d) based on a combined pool of training data.

The segmentation masks were used to quantify spatial patterns of OM patches (Fig. 4e, f). Subsequently, the segmentation mask were transferred to the original measurements to compare ion distributions between different segments (Fig. 4f). The particle segments used comprised the total projected image area of both mineral and associated OM patches whereas particles with an area of ≤0.05 μm^2 were excluded. When observing the particle sizes with electron microscopy and NanoSIMS (Fig. 4a, b), particles were found that were larger than expected according to the segmentation based on Stoke's law. This can be explained by varying densities due to associated OM as well as the non-spherical shape of particles (Konert and Vandenberghe, 1997; Laird, 2001).

The coverage of particles with OM was calculated as the proportion of the total projected OM segment area from the total particle area as

$$\bar{C} = \frac{\sum_{i=1}^{N_p} \sum_{j=1}^{N_o} O_{ij}}{\sum_{i=1}^{N_p} P_i} \quad (1)$$

where N_p denotes the number of particles with label i, N_o denotes the number of organic patches with label j, O_{ij} denotes the size of an individual SOM patch [μm^2] and P_i denotes the size of a particle [μm^2].

The OM segmentation mask was used to compute a connectivity index of the OM patches of each individual particle. The dimensionless connectivity Γ_i (Renard and Allard, 2013; Schlüter et al., 2014) of the OM patches was calculated as

$$\Gamma_i = \frac{\sum_{j=1}^{N_o}(O_{ij}{}^2)}{\left[\sum_{j=1}^{N_o} O_{ij}\right]^2} \quad (2)$$

The OM connectivity index of a particle between 0 and 1 is increasing for more connected structures and decreasing for patchy structures with more isolated SOM patches on the same particle (Fig. 4f).

The average connectivity at a certain time after glacial retreat (Study I) or at a certain clay content (Study II) was computed by accounting for the varying sizes of the individual particles. The area-weighted mean (Schumaker, 1996) of connectivity was calculated according to

$$\bar{\Gamma} = \sum_{i=1}^{N_p}\left(\frac{O_i \times \Gamma_i}{\sum_{i=1}^{N_p} O_i}\right) \quad (3)$$

To analyze the chemical composition of individual OM patches, normalized CN:C ratios ($^{12}C^{14}N^-$: ($^{12}C^{14}N^- + {}^{12}C^-$)) of individual OM segments were calculated (Fig. 4f). The average CN:C ratio of a sample was computed as arithmetic mean of all OM patches in that sample as well as a mean of subdivisions of OM segment sizes. These elemental ratios obtained by a NanoSIMS offer insights into the relative spatial distributions of C and N (Alleon et al., 2015), whereas they differ from a C:N ratio obtained by an elemental analyzer.

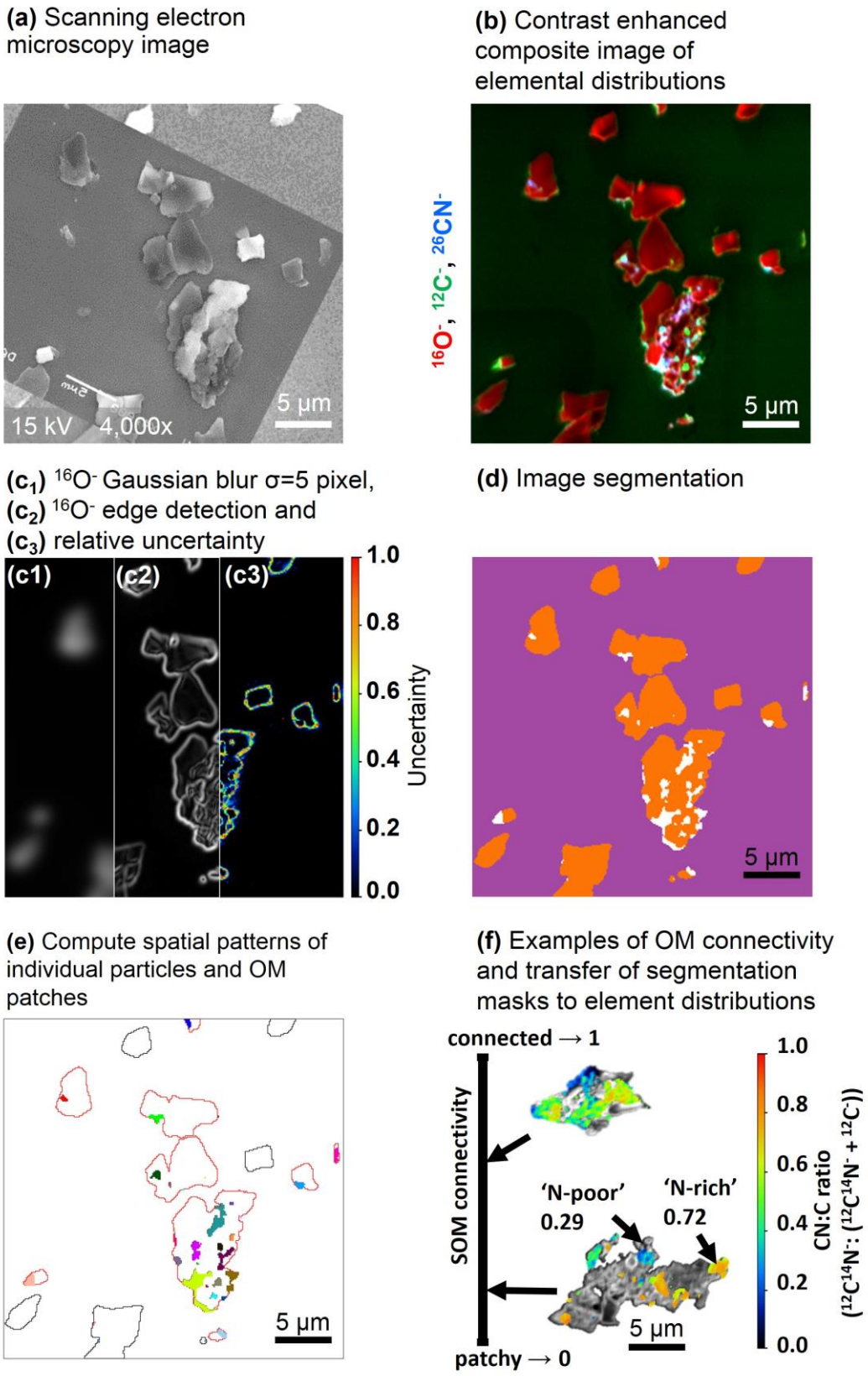

Fig. 4: Workflow of microscale investigations. (a) Localize regions of interest to (b) measure with NanoSIMS. (c) Employ multichannel machine-learning based algorithm to (d) segment image into background, mineral surfaces and OM patches. (e) Derive spatial patterns based on individual particle and OM segments (red/black outline for particles with/without OM patches) and (f) transfer segmentation mask to elemental ratios (modified according to data from Study I).

2.3.3 Morphological analysis by optical microscopy and microtomography (Study IV)

To gain morphological insights into the structure of microaggregates, the dry-crushed size fractions were analyzed using an optical Axio Imager M2 microscopy (Zeiss). Based on selected representative microaggregates from dry-crushed size fractions, computed microtomography was done by V.J.M.N.L. Felde at the University of Kassel (Germany) using an Xradia 520 Versa (Zeiss). With an acquisition time of 3 s, 1600 projections were obtained during rotation of the microaggregates, with a voxel resolution of 482–656 nm.

2.3.4 Size distribution of wet-sieved and dry-crushed microaggregates (Studies III and IV)

The size distributions of both wet-sieved and dry-crushed fractions were determined by dynamic image analysis in the Studies III and IV. This technique enabled detecting fine size changes of particles and aggregates at a resolution of several μm. In a QICPIC machine (Sympatec GmbH) at the Chair of Soil Ecology at the University of Freiburg (Germany), the size fractions were either pumped through the imaging unit as suspensions in a closed cycle (Fig. 5a, b) or analyzed in dry state with a drop tower under a constant flow of compressed air (Fig. 5d, e). In the imaging unit, a high-speed camera recorded the bypassing objects with rear illumination from a pulsed laser light (450 fps) at a resolution of several μm. The particle sizes in the recorded images were automatically computed using the minimum Feret diameter, which describes the minimum distance between two parallel tangents to the contour line of the objects (Allen, 1981) (Fig. 5c). To prevent air bubbles and root hairs from influencing the size distributions, the circularity of objects was set to be 0.6–0.93 based on individual object images reviewed within the internal WINDOX analysis software (Sympatec GmbH). The circularity is an index between 0 and 1 according to the ratio of the perimeter of a circle with an equivalent area to the measured object perimeter. Based on measured surface projections and an assumed density of 2.65 g cm^{-3}, the size distributions were computed as volumetric Q3 distribution (ISO 9276-1: 1998) to approximate a mass distribution as measured by sieving. To compare size distributions statistically, the median diameter was used. The size distributions were computed according to the mass contribution of the respective size fraction to the bulk soil.

The size distributions of objects in free and occluded microaggregate-sized fractions were determined for Study III with suspensions obtained after wet sieving and sonication as described previously in 2.2.4, whereas only a 250-μm sieve was used. To determine the size distributions of dispersible particles in the fractions, they were dispersed by shaking with 1 M $Na_4P_2O_7$ followed by sonication at 60 J ml^{-1}. Such dispersion enabled comparative analyses

of the mass contribution and size distribution of primary particles in the fractions (Kemper and Koch, 1966; Murer et al., 1993). To provide more details on the size distribution in the size range <11 µm, in which some particles might have been below the optical limits and not detected during the dynamic image analysis, sedimentation and pipette analysis was used. The size distributions <11 µm obtained by sedimentation and pipette analysis were merged with the size distributions of 11–250 µm by dynamic image analysis based on their mass contributions to the total size fraction <250 µm. The total size distribution was scaled according to its mass proportion in the bulk soil. The change of the size distributions after dispersion was used to identify specific size ranges of aggregates that dispersed into smaller particles. When calculating the difference of wet-sieved minus dispersed size distributions, a positive difference indicates aggregates, a negative difference indicates dispersed primary particles and unaggregated particles would be zero as they would remain undispersed (Fig. 6).

To determine the size distributions of the dry-crushed size fractions 20–53 µm and 53–250 µm in Study IV, a drop tower with a height of 50 cm was used to channel all objects towards the front of the optical imaging unit of the dynamic image analysis. A constant flow of compressed air helped to induce a constant flow of objects towards the imaging unit. To obtain further information about the water-stable and dispersible objects in the size fractions, the dry-crushed aggregates were also analyzed as suspensions with deionized H_2O and 0.1 M $Na_4P_2O_7$ as described previously. This also provided further insights into whether the failure mechanisms were different between the breakdown during dry crushing and the dispersion during wet sieving. The total size distribution <250 µm was merged based on the mass contributions and size distributions of both size fractions, 20–53 µm and 53–250 µm.

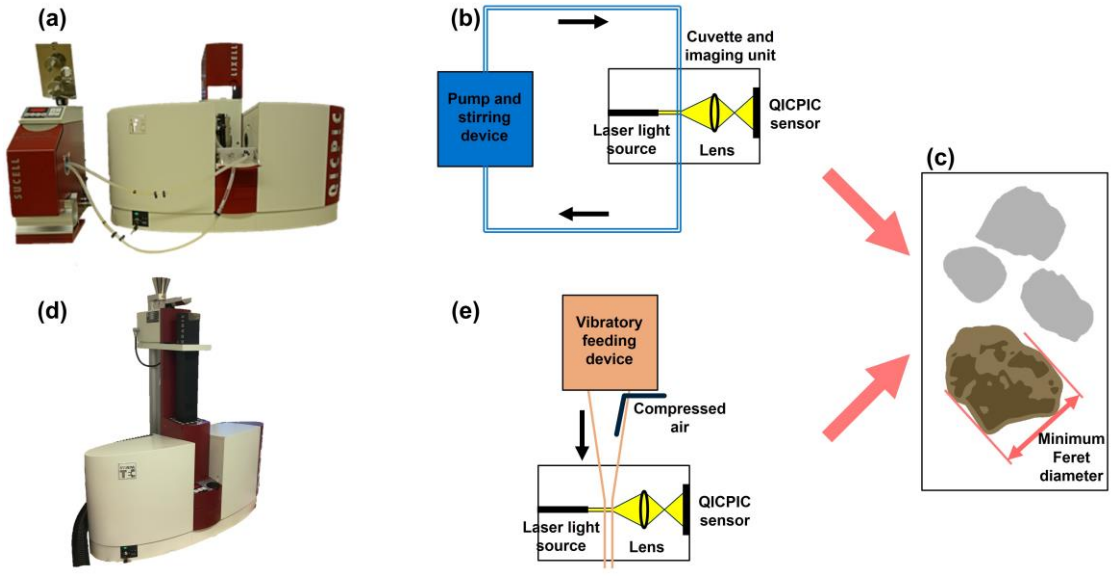

Fig. 5: Photos and schemes of two setups to determine the size distributions using dynamic image analysis. (a, b) Wet-sieved size fractions and (d, e) dry-crushed size fractions in the size range of microaggregates <250 µm. (c) Minimum Feret diameter as derived from the recorded images.

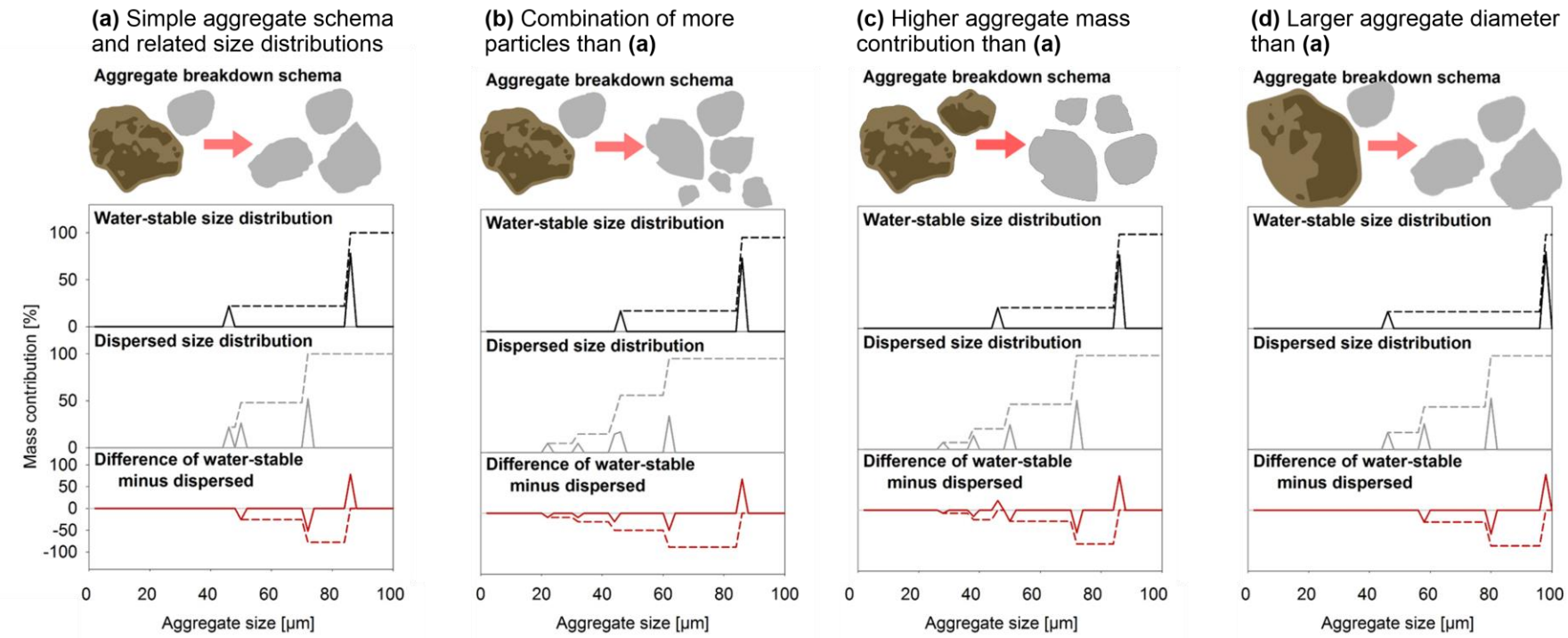

Fig. 6: Simplified theoretical scenarios of distinct aggregate mechanisms that occur simultaneously during aggregation. The size distributions shown as frequency mass contribution (solid line) and cumulative mass contribution (dashed line) are derived from measurements of a size fraction after wet sieving and dispersed state. The difference of wet-sieved minus dispersed size distribution enables detecting true aggregates (positive values), the building units of these aggregates (negative values), whereas non-aggregated particles are zero. This provides information about preferential size ranges of aggregates, the sizes of the building particles and the magnitude of aggregation within size fractions. (a) Simple case of one aggregate and one non-aggregated particle. Modifications of (a) illustrate three different types of aggregate forms: (b) as combination of more particles, (c) with higher aggregate mass contributions and (d) with larger aggregate diameter.

2.4 Statistical analyses

In Study I, RStudio 0.99 (RStudio Team, 2015) was used as a statistical tool to compute averages and standard errors for the spatial indices and to compile the results of the image analysis. When evaluating spatial indices of replicable spatial segments like individual particle sizes, OM patch sizes or the CN:C ratios, the normal distribution and homogeneity of variances was tested. To test whether means differed significantly, a one-way analysis of variance (ANOVA) with Tukey's honest significant difference test was used to compute pairwise differences.

In Studies II–IV, the relationships between clay content and OC contributions as well as concentrations were analyzed using Sigmaplot 11, including the verification of normality and equal variances, ANOVA and the application of a Tukey honest significant difference test to compare the means, if ANOVA was significantly different ($p<0.05$). In Study II, linear and logarithmic regression models were fitted according to their adjusted R^2. To analyze the relation between clay content and mineral-associated OC concentrations of fine OM fractions in Study II, an inverse first-order regression was used enabling the calculation of an asymptotic minimum OC concentration. In Study III, the relationship between the clay content and the mass contribution of size fractions or the mean aggregate size was evaluated using a linear model in R (RStudio 1.1.447) that incorporated the disparate spatial scales of the radial sampling schema with a nested site factor (Webster and Lark, 2013). The alkyl:O/N-alkyl ratio in Study III was analyzed with a two-factorial analysis testing the clay content, size fractions and their interaction.

3 Results and discussion

3.1 Initial soil formation related with successional establishment of OM patches at the microscale

To study the formation of soil microaggregates, the chronosequence approach of Study I offered insights into the initial formation of soil structures at the microscale in the Damma glacier forefield (Study I, Fig. 7). The soil structure formation in the forefield of the Damma glacier is driven by organo-mineral associations of mineral surfaces developing through mineral weathering of glacial deposits (Dümig et al., 2011) and the OM input derived from the establishing vegetation and biological activity (Schulz et al., 2013). At all time steps, clay-sized mineral particles account for approximately 55 % of the bulk soil OC as shown by Dümig et al. (2012). In Study I, an additional density fractionation of the clay-sized fraction revealed increasing mass proportions of the light clay-sized fraction (1.6–2.2 g cm^{-3}) at the expense of the heavy clay-sized fraction (>2.2 g cm^{-3}) (Study I, Fig. 1). The increasing proportion of the light clay-sized fraction, which contained more OM than the heavy clay-sized fraction, shows that the sequestration of OM on mineral surfaces occurred more rapidly with time after glacial retreat than the development of fresh mineral surfaces (Study I, Table 1). The increasing OC concentrations in the clay-sized fraction demonstrate that the sequestration of OM on mineral surfaces drives a rapid structural arrangement and formation of soil microaggregates at a decadal timescale. These observations corroborate previous experiments with artificial soil components, which stimulated an increasing initial microaggregate formation over several months (Pronk et al., 2017, 2012). The rapid soil formation dominated by OM sequestration in the Damma forefield provided a suitable chronosequence to further investigate the mechanisms of organo-mineral associations at the microscale.

The novel image analysis of Study I (Fig. 4) enabled to relate the increasing OM concentrations in the heavy and light clay-sized fractions with the arrangement of OM accrual over time of initial soil formation. Spatial patterns of OM accrual at the microscale could be quantified by multichannel machine-learning segmentation of NanoSIMS measurements (Fig. 4). This revealed successional stages with a rapid establishment of OM patches during the first decades. In later stages, the rate of OM coverage slowed down and the mineral surface was not masked completely in the mature soil (>700 years). This demonstrates that the soil OM is arranged at specific mineral surface sites, initially provided by clay-sized mineral particles (Dümig et al., 2012), at which the patchy-distributed OM developed into more connected structures (Study I, Fig. 3). These insights provide direct evidence for the development of mineral-associated OM over time in an environmental gradient of initial soil formation at the

microscale expanding previous observations of the patchy-distributed arrangement of OM by various techniques (Chenu and Plante, 2006; Ransom et al., 1997; Remusat et al., 2012; Vogel et al., 2014; Wagai et al., 2009). In a 6 weeks incubation experiment following the microspatial arrangement of OM in a soil, a preferential attachment of the added stable isotope labelled litter at pre-existing OM patches was observed (Vogel et al., 2014). Over time, a preferential attachment of OM suggests the in-situ expansion of mineral-associated OM over time, which slowed down during later stages of soil formation in the Damma forefield (Study I). The patchy-distributed OM provides potential linkage sites for the formation of larger microaggregate structures. The self-organized arrangement of OM-rich microdomains was observed by analyzing spatial patterns of elemental distributions within an intact macroaggregate (Steffens et al., 2017). In the same study, OM associated with phyllosilicates was distributed across the whole macroaggregate independent of recurring types of microarchitectures. The SSA of the clay-sized fractions in the Damma forefield decreased strongly during the initial stages and decreased slower at later stages of soil formation (Dümig et al., 2012). This indicates that the increasing coverage of minerals with OM observed by NanoSIMS is initially related with reactive mineral surfaces that are less important later. The initial establishment of specific mineral surface sites and the developing arrangement of patchy-distributed OM at these sites is intrinsically linked with the formation of soil microaggregates over time.

Mineral-associated OM is derived from microbial compounds and plant litter which are subject to microbial processing decreasing its C:N ratio (Baldock et al., 1997; Kallenbach et al., 2016; Pronk et al., 2013). Various factors can influence mineral-associated OM, like mineral surface reactivity (Mikutta et al., 2019; Pronk et al., 2013; Vogel et al., 2015; Yeasmin et al., 2017), microbial turnover (Cotrufo et al., 2013; Manzoni et al., 2012; Sollins et al., 2009), molecular properties (Kleber et al., 2007; Sollins et al., 2006) as well as the arrangement of OM at the microscale (Kleber et al., 2007; McCarthy et al., 2008; Vogel et al., 2014). Especially N-rich compounds were advocated to be associated with mineral surfaces (Kopittke et al., 2020, 2018) and provide gluing capacity for the formation of soil microaggregates (Kleber et al., 2015). When investigating the initial soil formation in Study I, the distribution of N-rich compounds across OM patches reflected the conceptual understanding of ecosystem succession over time in the same glacial forefield (Study I, Fig. 4). After an initial period of N assimilating species (Esperschütz et al., 2011; Zumsteg et al., 2012), N-demanding species succeed after several decades (Ollivier et al., 2011; Schulz et al., 2013). Species turning over N from the biomass and using it for nitrification and denitrification become active at later stages (Brankatschk et al., 2011; Tscherko et al., 2004). Based on the image analysis in Study I, it was observed that the individual OM patches retained more N-rich compounds, in relation to the C distribution, after

several decades than compared to the initial and mature soil stage. This suggests a dynamic relation of the ecological succession with the C and N composition of OM patches at the microscale, where the patchy distribution of OM patches likely reflects microbial habitats. Further studies are needed to resolve the effect of microbes on mineral-associated OM at the microscale by correlating techniques and relating their habitat distribution with the measurement of chemical properties.

The correlation of spatial patterns observed through image analyses like in Study I offers novel opportunities to resolve driving factors underlying the heterogeneous distribution of OM patches at the microscale. This enables research approaches to collect novel data on the spatial arrangement and better understand whether there is a preferential type of mineral surface associated with OM sequestration, if OM and mineral surface undergo compositional changes when associated, in which way microbes play a role in the conditioning of surfaces and the association of OM and how indices of stability and turnover of organo-mineral associations can be quantified. Studies for which the newly developed image analysis protocol was already implemented successfully include (i) the differentiation of zones with distinct Fe, Al and OM composition in close proximity of rice root cells (Kölbl et al., 2017), (ii) the quantification of microspatial correlations of Fe and Al associations with OM in a Hawaiian rainfall gradient (Inagaki et al., 2020) and (iii) direct evidence for larger aggregate diameters through bacteria as well as a sheltering effect of the microaggregates on bacteria when exposed to desiccation stress (Krause et al., 2019). All microscale observations in these studies are characterized by a specific structural arrangement, that was quantified by size, distance or a distinct elemental composition. After its formation, such specific soil microarchitecture exerts a major control over soil processes, since it determines the location and surroundings of organic and mineral soil components and whether their potential properties are applied.

3.2 Organic matter distribution and arrangement decoupled from clay content

While Study I revealed that the initial arrangement of OM in microstructures enables the rapid accrual of OM and does not appear to be limited by the slower development of fine particle surfaces, the Studies II and III elucidated the role of fine mineral particles further. For the Studies II and III, samples from a clay content gradient on an agricultural research site in SE Germany enabled analyses of arable soils with varying fine mineral particle proportions. The distribution and composition of OM was analyzed by density fractions in Study II and size fractions in the range of microaggregates in Study III. Across the wide clay content gradient of

5–37 % clay, we found similar bulk OC concentrations. This is in contrast to established concepts, that link an increased content of fine mineral surfaces with an increased sequestration of OM (Carter et al., 2003; Feng et al., 2014; Hassink, 1997; Stewart et al., 2008, 2007). This model concept is based on a hypothetical 'protective capacity' of OM through clay-sized and silt-sized particle fractions and parameterized according to the mass proportions of fine mineral particles in the bulk soil (Campbell and Paustian, 2015; Paustian et al., 1992; Stewart et al., 2007). The correlations of mass contributions of fine mineral soil particle fractions with their OC contributions to the bulk soil involved samples from different horizons, climatic conditions, parent material or land management. This could confound the relationship of fine mineral particles with their OM contributions. The clay content gradient of Study II offers a unique study site properties, since all samples were taken from one agricultural research site with a comparable crop management during several decades of documented agricultural management (Schröder et al., 2002). The differences of OC concentration changes of density fractions across the clay content gradient prevail in comparison with minor increases in the potential C input (Study III, 2.1) and slight variations of the illitic clay mineral composition (Study II, Supp. Table 1). These general conditions of the clay content gradient used in Study II allow a relatively isolated analysis of the influence of fine mineral particles on the OM sequestration in soil fractions under arable management.

Despite the similarities of the bulk soil OC concentrations across the 5–37 % clay content gradient, the density fractions revealed a high importance of OM sequestration by association with minerals in soils with lower clay contents and an increasing importance of the occlusion of particulate OM in soils with higher clay contents. In the isolated mineral-associated fine fractions (>1.8 g cm^{-3}) the low-clay soils (5–18 %) were found to contain increasing concentrations of OC with decreasing clay content (Study II, Fig. 1c). The OC concentration of mineral-associated fractions <6.3 μm decreased from 70 mg g^{-1} at 6 % clay to <35 mg g^{-1} at clay contents >30 %. In the top 20 cm of the soil, this corresponds to 28 Mg OC ha^{-2} associated with fine minerals at 6 % clay content and 16 Mg OC ha^{-2} at 18–35 % clay (Study II, Fig. 2). When comparing the OC concentrations of fine mineral fractions <6.3 μm, OC was equally distributed to the fine silt-sized fraction 2–6.3 μm, the coarse clay-sized fraction 0.2–2 μm and the fine clay-sized fraction <0.2 μm despite their differences in total SSA (12.1 m^2 g^{-1}, 37.3 m^2 g^{-1} and 80.6 m^2 g^{-1} respectively). These observations of equal distribution of OM to fine mineral fractions demonstrate that there is no preferential OM distribution to the fraction with the highest SSA indicating that the OM distribution is decoupled from mineral surface area. Measurements of the OM accretion per mineral surface area have shown that the SSA occupied by OM is similar for both the coarse clay-sized and the fine silt-sized fraction

independent of the clay content (Study II, Fig. 1d). Despite the similar SSA occupied by OM, the higher OM contents in the fine fractions of the low-clay soils demonstrate a piled-up arrangement of the OM assemblages. When comparing the OM piled-up per mineral surface with monolayer-equivalent OC loadings from fine-textured marine sediments and upland soils (approximately 1 mg OC m^{-2}) (Keil et al., 1994; Mayer, 1994), 2-fold to 4-fold higher values were found in the coarse clay-sized fraction and 6-fold to 10-fold values in the fine silt-sized fraction (Study II, Fig. 1d). These results provide direct evidence for an arrangement of OM in piled-up assemblages as a result of earlier observations of the patchy distribution of OM across a minor proportion of mineral surfaces (Chenu and Plante, 2006; Ransom et al., 1997), the preferential attachment of litter-derived OC at pre-existing OM surfaces (Vogel et al., 2014) and the conceptual arrangement of adsorbed layers of organic molecules (Kleber et al., 2007; Sollins et al., 2006). In a previous study investigating the energy of the N_2 adsorption to the mineral surface across a gradient of soils with various OM contents, a so-called 'globular form' of organo-mineral association was postulated, whereas a 'painted form' was found for some subsurface horizons with low OM content and high SSA (Wagai et al., 2009). A preferential attachment of organic molecules with a 'globular' arrangement at goethite surfaces was observed using atomic force microscopy (Kaiser and Guggenberger, 2007). In a sorption experiment using dissolved OM and various soil-like mineral surfaces, a successive layering of OM with compositional changes was observed (Mitchell et al., 2018). Neutron reflectometry measurements of deposited glucose and stearic acid layers on soil-like aluminum oxide mineral surfaces revealed distinct layers driven by thermodynamic factors (Mayes et al., 2013; Petridis et al., 2014). The results of Study II demonstrate that mechanisms similar to these earlier observations of a globular or voluminous arrangement of OM can lead to increased accrual of OM on the same mineral surface area. As outlined in Study II, this leads to the conceptual notion that OM is arranged within a three-dimensional house-of-cards structure of fine mineral soil components, build up by edge-to-face interactions of fine mineral soil components and partly filled with OM (Study II, Fig. 4; Fig. 7b). The conceptual house-of-cards arrangement provides a compartmentalized scaffolding for a high proportion of mineral surfaces that was not covered with OM and the accumulation of OM in clustered patches (Fig. 7b).

The globular extension of OM through piled-up assemblages in Study II implies a different perspective compared to the surface extension of OM through increased OM coverage at mineral surfaces in Study I. Both Studies I and II show that OM sequestration is concentrated at a minor proportion of mineral surfaces within fine mineral particle fractions, whereas a piled-up arrangement reveals that such a concentration of OM at specific mineral sites does not limit the capacity to sequester OC in soil. This indicates that fine mineral particle fractions provide

important key sites for the sequestration of patchy-distributed OM without predetermining OM accrual since more OM can be accommodated in three-dimensional arrangements. Such sequestration of OM in voluminous structures provides additional explanation for earlier experiments, which observed OC concentrations higher or more variable than predicted by the 'protective capacity' of fine mineral particles (Feng et al., 2013; Heitkamp et al., 2012; Yang et al., 2016; Zhao et al., 2006). Despite these variable results, the mass proportion of fine mineral particles is widely used to predict OM concentrations of soils using biogeochemical modelling approaches (Campbell and Paustian, 2015; Di et al., 2018; Stewart et al., 2007). The results of Studies I and II challenge the assumptions underlying such modelling efforts and indicate a higher potential to stabilize OM than predicted through mineral surface area, whereas OM-OM interactions are likely to influence OM accrual through spatial arrangement. This implies that some OM conceptualized as mineral-associated is actually governed by organo-organo interactions. This could explain why anticipated correlations between soil mineral composition and OM contents were not found in several earlier studies (Fernández-Ugalde et al., 2016; Pronk et al., 2013; Wattel-Koekkoek et al., 2001). The spatial arrangement of OM governs the accessibility of preferred OM surfaces and reactive mineral surfaces for the stabilization of fresh OM in the system. A compartmentalized and preferential binding of OM at distinct surface sites suggests that OM sequestration does not mask reactive mineral surfaces that retain functions like the storage and exchange of nutrients and water (Fig. 7b).

3.3 Wet-sieved microaggregate diameters and occlusion of particulate organic matter mediated by clay content

The combined arrangement of various soil components during aggregation can determine whether individual or interactive properties of the building particles become effective within the architectures of microaggregates. Since many aggregation studies employ the isolation of size fractions, underlying patterns on the proportion of aggregates in these size fractions, how building particles are combined within aggregates and the size distribution of the aggregates remain mostly unresolved. To unravel these interactions, a novel approach differentiating the size distributions of soil fractions <250 μm from their dispersible particle size distributions was developed in Study III using dynamic image analysis. This approach provided information about preferential size ranges of aggregates and particles at a resolution of several μm. The application of this approach to samples from the Scheyern gradient of 16–37 % clay content allowed the analysis of potentially different size compositions of particles that build microaggregates. An earlier density fractionation study of size fractions <53 μm postulated a

constant ratio of silt-sized to clay-sized particles for true microaggregates (Balabane and Plante, 2004). The results of Study III showed that free water-stable microaggregates of approximately 30 μm diameter dominated the size distributions in the soils despite differences in soil texture or mass proportion of the size fractions in the bulk soil (Study III, Fig. 3). Independent of the soil texture, microaggregates with a diameter of 30 μm seem to be a predominant architecture that remained stable after wet sieving (Study III, Fig. 7a). However, for aggregate diameters >50 μm, a stabilizing effect of clay content on water-stable aggregates was found. In the size range 50–180 μm the mean aggregate size was 11 μm larger in the soils with higher clay content (Study III, Table 2). With increasing clay content, the mass proportion of water-stable macroaggregates >250 μm increased, which were found to contain a 4 % higher clay content (Study III, Fig. 4). It was also found that sand-sized particles >100 μm did not form part of water-stable aggregates and might, therefore, have hampered the buildup of larger aggregate structures within the soil matrix of the low-clay soils (Study III, Fig. 7a).

Along the clay content gradient of Study II, we found increasing proportions of OC in particulate OM occluded in aggregates. Although the high-clay soils provided more surface as potential binding capacity for OM, the increased amount of clay-sized mineral particles stabilized more aggregates that occlude additional particulate OM. Instead of a direct effect through sorption, this demonstrates that fine mineral particles can indirectly exert control over OM sequestration through stabilizing larger soil microaggregates as shown in Study III. This corroborates several studies which directly observed the arrangement of phyllosilicates around particulate OM within aggregate architectures at the microscale (Steffens et al., 2017; Watteau et al., 2012). The dense occlusion of fine mineral particles around particulate OM make it an important nucleus for aggregation as shown in two studies using artificial soil components (Bucka et al., 2019; Pronk et al., 2012) and hamper the decomposition of the OM (McCarthy et al., 2008; Rabbi et al., 2020; Virto et al., 2010). The influence of soil texture on OM sequestration can be concluded to become effective indirectly through aggregate architectures and the structural arrangement of fine and coarse mineral particles instead of direct surface interactions. Accordingly, the stabilization of microaggregate structures as a whole prevailed over a direct sorptive stabilization of OM with increasing soil clay content. Since the analyses in Studies I and II showed that the sequestration of mineral-associated OM is decoupled from a majority of the reactive mineral surface area, the stabilization of microaggregates could be more related to an increased aggregation of the soil mineral particles along with a potentially more effective occlusion of (particulate) OM, as indicated by the conceptualized house-of-cards structure (Fig. 7b).

3.4 Dry crushing isolates soil microaggregates influenced by soil texture

The dynamic image analysis of dry-crushed size fractions <250 μm provided insights into size distribution of aggregates and particles at a resolution of several μm (Fig. 5b). To analyze the effect of the microaggregate isolation methods, the results from dry-crushed fractions in Study IV were compared with the data on wet-sieved fractions in Study III. The comparison of three soils with different clay contents (19, 24 and 34 %) revealed a bimodal size distribution with preferential diameters at 50 and 150 μm (Study IV, Fig. 4). The aggregates in the soil with 34 % clay were smaller than the other soils with lower clay contents (Study IV, Table 1), due to the smaller primary particles reflecting a mechanical breakdown along numerous failure planes during dry crushing. When compared with wet-sieved aggregates in Study III, the mean aggregate diameters of dry-crushed fractions in Study IV were larger. In this comparison, it can be observed that the relation of the clay content gradient with the size distributions depended on the isolation method. While the dry-crushed fractions were of up to approximately 40 μm larger diameter in the soils with lower clay content (Study IV, Table 1), the wet-sieved aggregates were of up to approximately 10 μm larger diameter in the soils with higher clay content (Study III, Table 2). These differences are related with different failure mechanisms addressed by the compared isolation methods: Microaggregates are dispersed through slaking and differential swelling during wet sieving (Le Bissonnais, 1996), whereas the uniaxial compression force during dry crushing leads to a mechanical breakdown along planes of weaknesses (Kristiansen et al., 2006). These different aggregate failure mechanisms result in different microaggregate size distributions, which is strongly influenced by soil texture as quantified by dynamic image analysis in Studies III and IV. This also means that the extent of aggregate failure due to either breakdown or dispersion varies depending on the soil texture.

The larger diameter of microaggregates in dry-crushed fractions was related with more sand-sized primary particles of approximately 100–250 μm in diameter. Microscopy analysis and tomography scans demonstrated that these sand-sized particles are mostly found inside the dry-crushed aggregate structures (Study IV, Fig. 2), thereby increasing the aggregate diameter. In the wet-sieved fractions <250 μm in Study III, sand-sized particles of >100 μm diameter did not form part of wet-sieved microaggregates. These differences show that sand-sized primary particles can form a stable part of soil microaggregates when isolated by dry crushing, but are dispersed during wet sieving. To analyze the dispersion of dry-crushed microaggregates, the size fractions were subjected to wetting which resulted in a unimodal size distribution with a preferential diameter at approximately 25 μm (Study IV, Fig. 4b). This is similar to the

preferential aggregate diameter of 30 μm in the wet-sieved fractions of Study III. Both analyses show that aggregate structures which measured approximately 25–30 μm in diameter seem to be most water-stable independent of the soil texture (Fig. 7a). In contrast, the high influence of the clay content gradient on the microaggregate diameter and structure in dry-crushed fractions demonstrate that dry crushing can be recommended for research questions where intact microaggregate structures need to be isolated that contain all kind of primary particles including sand-sized ones. To reproduce uniaxial crushing, soil aggregates can also be isolated by crushing them vertically between two plates with a fixed minimum distance instead of using a whole loading frame.

The influence of the isolation methods on the structure of microaggregates also affects several properties, like the mechanical stability of individual aggregates as well as the OC concentrations and the bacterial community composition of the size fractions. The mechanical stability was higher and more variable in dry-crushed fractions compared with wet-sieved ones (Study IV, Fig. 5). This correlated with higher contents of sand-sized primary particles and OC concentrations in the dry-crushed fractions (Study IV, Fig. 6) which might have stabilized and increased the heterogeneity of the aggregate architecture leading to a more variable breakdown. When comparing soil from the clay content gradient, the OC concentrations in the dry-crushed fraction 53–250 μm increased with clay content. This was related with the sizes of primary particles in the microaggregates, since more sand-sized particles would occupy more space and lead to a lower OC concentration. The more heterogeneous architecture of aggregates in the dry-crushed fractions also led to a higher bacterial alpha diversity and different bacterial communities compared to wet-sieved fractions (Study IV, Fig. 7 and 8). It became clear, that the choice for a method to isolate soil microaggregates, like wet sieving or dry crushing, can greatly influence conclusions on the bulk soil based on aggregate fractions. The dispersion into fine microaggregates through wet sieving might be suitable for studies of OM dynamics, whereas the sandy microaggregates isolated by dry crushing might be more advantageous to study the microbial diversity while preserving sand-sized particles within the structural architecture of the aggregates.

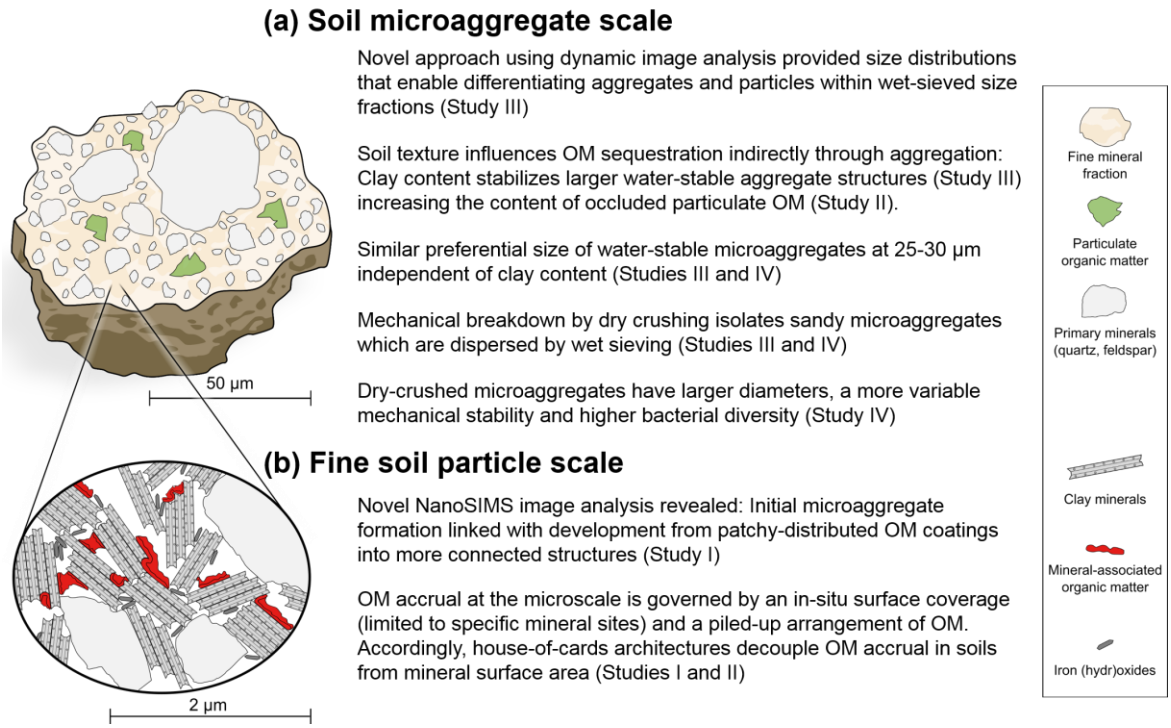

Fig. 7: Schematic conclusion of this work. Findings are summarized in a conceptual understanding at (a) the scale of microaggregates and (b) the scale of fine soil particles.

4 Conclusions and outlook

This thesis focused on the spatial arrangement of OM at the microscale, analyzed the influence of fine mineral particles on the distribution of mineral-associated OM and compared wet-sieved and dry-crushed microaggregates to find out how soil texture affects microaggregate structures depending on failure mechanisms (Fig. 7). The Damma chronosequence in Study I revealed a rapid initial formation of microaggregates by OM accrual, which is decoupled from the slower development rate of fine mineral surfaces produced during weathering. The novel image analysis approach enabled to quantify spatial patterns of OM distribution at the microscale in Studies I and II through the multichannel machine-learning segmentation of NanoSIMS measurements. This provided direct evidence of the tight relations between the initial formation of soil microaggregates and spatial patterns of patchy-distributed OM developing into more connected structures. The compositional changes of OM patches followed postulated ecosystem dynamics, which suggests a tight coupling between plants, microbes and OM patches at the microscale. Further studies are needed to incorporate the spatial arrangement of OM which will provide promising opportunities to further resolve driving factors of the formation, heterogeneous distribution and local turnover of OM patches at the microscale. Especially the microspatial correlation of OM distribution and microbial processes could be a next step to determine the co-localization of microbial activity with OM patches and analyze whether microbes can actively dominate over the influence of mineral mechanisms that stabilize OM.

Soils with low clay content (<18 %) sequester OM in an increasingly piled-up arrangement as shown in Study II. Such OM sequestration by voluminous extension adds a three-dimensional conception to the successional development and well-connected surface extension of OM patches in Study I (Fig. 7b). While most OM is initially arranged around fine mineral particle surfaces, ultimately OM sequestration is mostly decoupled from the specific mineral surface area. Taken together, Studies I and II show that OM is highly concentrated at specific surface sites in fine mineral particles whereas substantial amounts of OM are sequestered by piling instead of being limited to the mineral surface covered by OM. This led to the conceptual understanding of OM being arranged in a house-of-card structure that can accumulate OM via organo-organo interactions rather than only in association with mineral surfaces (Fig. 7b). Such architectures enable OM sequestration but do not limit it to a certain capacity. Future studies should investigate the surface properties responsible for the piled-up arrangement and the potential of these voluminous assemblages for the sequestration and turnover of OM. A potential next step would be to develop spatially resolved measures for the surface reactivity of mineral and organic surfaces and correlate these with the OM distribution, which provides

insights into a hypothesized preferability of newly associated OM and the potentially competitive influence of mineral and organic surfaces.

Fine mineral particles stabilize larger microaggregates and more macroaggregates as shown in Study III. This explains the increased proportions of occluded particulate OM found in the soils with higher clay content (>18 %) of Study II. The novel approach to differentiate the size distributions of true microaggregates within size fractions of Study III revealed that aggregates were predominantly present at a diameter of 30 μm after wet sieving independent of the clay content. Such fine sized aggregates might be a ubiquitous type of water-stable microaggregate architecture, whereas large sand grains >100 μm have hampered the build-up of larger aggregates >50 μm. Taken together, Studies II and III demonstrate how soil texture affects OM sequestration indirectly depending on aggregate architecture by the re-distribution of fine mineral particles into larger aggregates or around particulate OM.

The isolation method greatly influences the properties of fractionated soil microaggregates in relation with different failure mechanisms as shown in Study IV. The dynamic image analysis enabled detecting changes of microaggregate diameters and particles at the microscale. The mechanical breakdown during dry crushing isolates microaggregates that include sand-sized primary particles in soils with a lower clay content while wetting caused their dispersion into finer microaggregates. The inclusion of sand-sized primary particles in dry-crushed aggregates led to larger aggregate diameters, a more variable mechanical stability and a higher bacterial diversity. Accordingly, dry crushing can be recommended to isolate soil microaggregates while preserving the inclusion of large primary particles.

This work identified drivers of OM sequestration in soils at the microscale, like the successive surface coverage of OM patches over time and the piled-up arrangement of OM assemblages. These microspatial processes were related with the sequestration of OM at the scale of soil microaggregates as influenced by soil texture, aggregate diameters and isolation methods. All these processes control a heterogeneous spatial arrangement of OM and provide a leverage for the fate of OM in soil microstructures. A spatially resolved perspective on the stabilization of OM provides opportunities to detect where and under which conditions OM is locally stabilized in soils by mineral, microbial or molecular interactions.

5 References

Allen, T. (1981): Particle size measurement, in: Powder Sampling and Particle Size Measurement Methods. Chapmann & Hall, London.

Alleon, J., Bernard, S., Remusat, L., Robert, F. (2015): Estimation of nitrogen-to-carbon ratios of organics and carbon materials at the submicrometer scale. Carbon 84, 290–298. https://doi.org/10.1016/j.carbon.2014.11.044

Amelung, W., Zech, W. (1999): Minimisation of organic matter disruption during particle-size fractionation of grassland epipedons. Geoderma 92, 73–85.

Amelung, W., Zech, W., Zhang, X., Follett, R.F., Tiessen, H., Knox, E., Flach, K.-W. (1998): Carbon, Nitrogen, and Sulfur Pools in Particle-Size Fractions as Influenced by Climate. Soil Science Society of America Journal 62, 172–181. https://doi.org/10.2136/sssaj1998.03615995006200010023x

Amézketa, E. (1999): Soil aggregate stability: A review. Journal of Sustainable Agriculture 14, 83–151.

Angers, D.A., Recous, S., Aita, C. (1997): Fate of carbon and nitrogen in water-stable aggregates during decomposition of $^{13}C^{15}N$-labelled wheat straw in situ. European Journal of Soil Science 48.

Atterberg, A. (1917): Die Konsistenzlehre - Eine neue physikalische Lehre. Kolloid-Zeitschrift 20, 1–7.

Bach, E.M., Hofmockel, K.S. (2014): Soil aggregate isolation method affects measures of intra-aggregate extracellular enzyme activity. Soil Biology and Biochemistry 69, 54–62. https://doi.org/10.1016/j.soilbio.2013.10.033

Balabane, M., Plante, A.F. (2004): Aggregation and carbon storage in silty soil using physical fractionation techniques. European Journal of Soil Science 55, 415–427. https://doi.org/10.1111/j.1351-0754.2004.0608.x

Baldock, J.A., Oades, J.M., Nelson, P.N., Skene, T.M., Golchin, A., Clarke, P. (1997): Assessing the extent of decomposition of natural organic materials using solid-state 13C NMR spectroscopy. Soil Research 35, 1061–1084. https://doi.org/10.1071/S97004

Balesdent, J., Wagner, G.H., Mariotti, A. (1988): Soil Organic Matter Turnover in Long-term Field Experiments as Revealed by Carbon-13 Natural Abundance. Soil Science Society of America Journal 52, 118–124. https://doi.org/10.2136/sssaj1988.03615995005200010021x

Barré, P., Durand, H., Chenu, C., Meunier, P., Montagne, D., Castel, G., Billiou, D., Soucémarianadin, L., Cécillon, L. (2017): Geological control of soil organic carbon and nitrogen stocks at the landscape scale. Geoderma 285, 50–56. https://doi.org/10.1016/j.geoderma.2016.09.029

Barré, P., Fernandez-Ugalde, O., Virto, I., Velde, B., Chenu, C. (2014): Impact of phyllosilicate mineralogy on organic carbon stabilization in soils: incomplete knowledge and exciting prospects. Geoderma 235–236, 382–395. https://doi.org/10.1016/j.geoderma.2014.07.029

Bernasconi, S.M., Bauder, A., Bourdon, B., Brunner, I., Bünemann, E., Chris, I., Derungs, N., Edwards, P., Farinotti, D., Frey, B., Frossard, E., Furrer, G., Gierga, M., Göransson, H., Gülland, K., Hagedorn, F., Hajdas, I., Hindshaw, R., Ivy-Ochs, S., Jansa, J., Jonas, T., Kiczka, M., Kretzschmar, R., Lemarchand, E., Luster, J., Magnusson, J., Mitchell, E.A.D., Venterink, H.O., Plötze, M., Reynolds, B., Smittenberg, R.H., Stähli, M., Tamburini, F., Tipper, E.T., Wacker, L., Welc, M., Wiederhold, J.G., Zeyer, J., Zimmermann, S., Zumsteg, A. (2011): Chemical and Biological Gradients along the Damma Glacier Soil Chronosequence, Switzerland. Vadose Zone Journal 10, 867. https://doi.org/10.2136/vzj2010.0129

Bimüller, C., Kreyling, O., Kölbl, A., von Lützow, M., Kögel-Knabner, I. (2016): Carbon and nitrogen mineralization in hierarchically structured aggregates of different size. Soil and Tillage Research 160, 23–33. https://doi.org/10.1016/j.still.2015.12.011

Biscaye, P.E. (1965): Mineralogy and sedimentation of recent deep-sea clay in the Atlantic ocean and adjacent seas and oceans. Bulletin of the Geological Society of America 76, 803–832. https://doi.org/10.1130/0016-7606(1965)76[803:MASORD]2.0.CO;2

Blaud, A., Menon, M., van der Zaan, B., Lair, G.J., Banwart, S.A. (2017): Effects of Dry and Wet Sieving of Soil on Identification and Interpretation of Microbial Community Composition, in: Advances in Agronomy. Elsevier, pp. 119–142. https://doi.org/10.1016/bs.agron.2016.10.006

Bosatta, E., Ågren, G.I. (1997): Theoretical analyses of soil texture effects on organic matter dynamics. Soil Biology and Biochemistry 29, 1633–1638. https://doi.org/10.1016/S0038-0717(97)00086-2

Brankatschk, R., Towe, S., Kleineidam, K., Schloter, M., Zeyer, J. (2011): Abundances and potential activities of nitrogen cycling microbial communities along a chronosequence of a glacier forefield. ISME J 5, 1025–1037.

Brunauer, S., Emmett, P.H., Teller, E. (1938): Adsorption of Gases in Multimolecular Layers. Journal of the American Chemical Society 60, 309–319. https://doi.org/10.1021/ja01269a023

Bucka, F.B., Kölbl, A., Uteau, D., Peth, S., Kögel-Knabner, I. (2019): Organic matter input determines structure development and aggregate formation in artificial soils. Geoderma 354, 113881. https://doi.org/10.1016/j.geoderma.2019.113881

Burke, I.C., Yonker, C.M., Parton, W.J., Cole, C.V., Flach, K., Schimel, D.S. (1989): Texture, Climate, and Cultivation Effects on Soil Organic Matter Content in U.S. Grassland Soils. Soil Science Society of America Journal 53, 800–805. https://doi.org/10.2136/sssaj1989.03615995005300030029x

Campbell, E.E., Paustian, K. (2015): Current developments in soil organic matter modeling and the expansion of model applications: a review. Environmental Research Letters 10, 123004. https://doi.org/10.1088/1748-9326/10/12/123004

Carroll, D. (1959): ION EXCHANGE IN CLAYS AND OTHER MINERALS. GSA Bulletin 70, 749–779. https://doi.org/10.1130/0016-7606(1959)70[749:IEICAO]2.0.CO;2

Carter, M.R., Angers, D.A., Gregorich, E.G., Bolinder, M.A. (2003): Characterizing organic matter retention for surface soils in eastern Canada using density and particle size fractions. Canadian Journal of Soil Science 83, 11–23. https://doi.org/10.4141/S01-087

Chabbi, A., Lehmann, J., Ciais, P., Loescher, H.W., Cotrufo, M.F., Don, A., SanClements, M., Schipper, L., Six, J., Smith, P., Rumpel, C. (2017): Aligning agriculture and climate policy. Nature Climate Change 7, 307. https://doi.org/10.1038/nclimate3286

Chaplot, V., Cooper, M. (2015): Soil aggregate stability to predict organic carbon outputs from soils. Geoderma 243–244, 205–213. https://doi.org/10.1016/j.geoderma.2014.12.013

Chenu, C., Plante, A.F. (2006): Clay-sized organo-mineral complexes in a cultivation chronosequence: revisiting the concept of the "primary organo-mineral complex." European Journal of Soil Science 57, 596–607. https://doi.org/10.1111/j.1365-2389.2006.00834.x

Christensen, B.T. (2001): Physical fractionation of soil and structural and functional complexity in organic matter turnover. European Journal of Soil Science 52, 345–353. https://doi.org/10.1046/j.1365-2389.2001.00417.x

Christensen, B.T. (1992): Physical fractionation of soil and organic matter in primary particle size and density separates. Advances in Soil Sciences 20, 1–90.

Churchman, G.J. (2018): Game Changer in Soil Science. Functional role of clay minerals in soil. Journal of Plant Nutrition and Soil Science 181, 99–103. https://doi.org/10.1002/jpln.201700605

Churchman, G.J. (2010): Is the geological concept of clay minerals appropriate for soil science? A literature-based and philosophical analysis | Elsevier Enhanced Reader. Physics and Chemistry of the Earth 35, 927–940. https://doi.org/10.1016/j.pce.2010.05.009

Cotrufo, M.F., Wallenstein, M.D., Boot, C.M., Denef, K., Paul, E. (2013): The Microbial Efficiency-Matrix Stabilization (MEMS) framework integrates plant litter decomposition with soil organic matter stabilization: do labile plant inputs form stable soil organic matter? Global Change Biology 19, 988–995. https://doi.org/doi:10.1111/gcb.12113

Dexter, A.R. (1988): Advances in characterization of soil structure. Soil and Tillage Research 11, 199–238.

Dexter, A.R., Kroesbergen, B. (1985): Methodology for determination of tensile strength of soil aggregates. Journal of Agricultural Engineering Research 31, 139–147. https://doi.org/10.1016/0021-8634(85)90066-6

Dexter, A.R., Richard, G., Arrouays, D., Czyż, E.A., Jolivet, C., Duval, O. (2008): Complexed organic matter controls soil physical properties. Geoderma 144, 620–627. https://doi.org/10.1016/j.geoderma.2008.01.022

Di, J., Xu, M., Zhang, W., Tong, X., He, X., Gao, H., Liu, H., Wang, B. (2018): Combinations of soil properties, carbon inputs and climate control the saturation deficit dynamics of stable soil carbon over 17-year fertilizaiton. Scientific Reports 8, 12653. https://doi.org/10.1038/s41598-018-31028-x

Dümig, A., Häusler, W., Steffens, M., Kögel-Knabner, I. (2012): Clay fractions from a soil chronosequence after glacier retreat reveal the initial evolution of organo–mineral associations. Geochimica et Cosmochimica Acta 85, 1–18. http://dx.doi.org/10.1016/j.gca.2012.01.046

Dümig, A., Smittenberg, R., Kögel-Knabner, I. (2011): Concurrent evolution of organic and mineral components during initial soil development after retreat of the Damma glacier, Switzerland. Geoderma 163, 83–94. http://dx.doi.org/10.1016/j.geoderma.2011.04.006

Ebrahimi, A., Or, D. (2018): On Upscaling of Soil Microbial Processes and Biogeochemical Fluxes From Aggregates to Landscapes. Journal of Geophysical Research: Biogeosciences 123, 1526–1547. https://doi.org/10.1029/2017JG004347

Edwards, A.P., Bremner, J.M. (1967): Microaggregates in soils. Journal of Soil Science 18, 64–73.

Elliott, E.T., Palm, C.A., Reuss, D.E., Monz, C.A. (1991): Organic matter contained in soil aggregates from a tropical chronosequence: correction for sand and light fraction. Agriculture, Ecosystems & Environment 34, 443–451. https://doi.org/10.1016/0167-8809(91)90127-J

Esperschütz, J., Welzl, G., Schreiner, K., Buegger, F., Munch, J.C., Schloter, M. (2011): Incorporation of carbon from decomposing litter of two pioneer plant species into microbial communities of the detritusphere. FEMS Microbiology Letters 320, 48–55. https://doi.org/10.1111/j.1574-6968.2011.02286.x

FAO (2014): World reference base for soil resources 2014: international soil classification system for naming soils and creating legends for soil maps. FAO, Rome.

Feller, C., Beare, M.H. (1997): Physical control of soil organic matter dynamics in the tropics. Geoderma 79, 69–116. https://doi.org/10.1016/S0016-7061(97)00039-6

Feller, C., Schouller, E., Thomas, F., Rouiller, J., Herbillon, A.J. (1992): N2-bet specific surface areas of some low activity clay soils and their relationships with secondary constituents and organic matter contents. Soil Science 153, 293–299. https://doi.org/10.1097/00010694-199204000-00005

Feng, W., Plante, A.F., Aufdenkampe, A.K., Six, J. (2014): Soil organic matter stability in organo-mineral complexes as a function of increasing C loading. Soil Biology and Biochemistry 69, 398–0405. https://doi.org/10.1016/j.soilbio.2013.11.024

Feng, W., Plante, A.F., Six, J. (2013): Improving estimates of maximal organic carbon stabilization by fine soil particles. Biogeochemistry 112, 81–93. https://doi.org/10.1007/s10533-011-9679-7

Fernández-Ugalde, O., Barré, P., Hubert, F., Virto, I., Girardin, C., Ferrage, E., Caner, L., Chenu, C. (2013): Clay mineralogy differs qualitatively in aggregate-size classes: clay-mineral-based evidence for aggregate hierarchy in temperate soils. European Journal of Soil Science 64, 410–422. https://doi.org/10.1111/ejss.12046

Fernández-Ugalde, O., Barré, P., Virto, I., Hubert, F., Billiou, D., Chenu, C. (2016): Does phyllosilicate mineralogy explain organic matter stabilization in different particle-size fractions in a 19-year C3/C4 chronosequence in a temperate Cambisol? Geoderma 264, 171–178. https://doi.org/10.1016/j.geoderma.2015.10.017

Field, D.J., Minasny, B. (1999): A description of aggregate liberation and dispersion in A horizons of Australian Vertisols by ultrasonic agitation. Geoderma 91, 11–26.

Ghezzehei, T.A., Or, D. (2000): Dynamics of soil aggregate coalescence governed by capillary and rheological processes. Water Resources Research 36, 367–379. https://doi.org/10.1029/1999WR900316

Golchin, A., Oades, J.M., Skjemstad, J.O., Clarke, P. (1994): Soil structure and carbon cycling. Soil Research 32, 1043–1068.

Gormanns, P., Reckow, S., Poczatek, J.C., Turck, C.W., Lechene, C. (2012): Segmentation of Multi-Isotope Imaging Mass Spectrometry Data for Semi-Automatic Detection of Regions of Interest. PLOS ONE 7, e30576. https://doi.org/10.1371/journal.pone.0030576

Graf-Rosenfellner, M., Cierjacks, A., Kleinschmit, B., Lang, F. (2016): Soil formation and its implications for stabilization of soil organic matter in the riparian zone. Catena 139, 9–18. https://doi.org/10.1016/j.catena.2015.11.010

Graf-Rosenfellner, M., Kayser, G., Guggenberger, G., Kaiser, K., Büks, F., Kaiser, M., Mueller, C.W., Schrumpf, M., Rennert, T., Welp, G., Lang, F. (2018): Replicability of aggregate disruption by sonication—an inter-laboratory test using three different soils from Germany. Journal of Plant Nutrition and Soil Science 181, 894–904. https://doi.org/10.1002/jpln.201800152

Gregorich, E.G., Kachanoski, R.G., Voroney, R.P. (1988): Ultrasonic dispersion of aggregates: Distribution of organic matter in size fractions. Canadian Journal of Soil Science 68, 395–403.

Hassink, J. (1997): The capacity of soils to preserve organic C and N by their association with clay and silt particles. Plant and Soil 191, 77–87.

Hatton, P.-J., Remusat, L., Zeller, B., Derrien, D. (2012): A multi-scale approach to determine accurate elemental and isotopic ratios by nano-scale secondary ion mass spectrometry imaging. Rapid Communications in Mass Spectrometry 26, 1363–1371. https://doi.org/10.1002/rcm.6228

Heckman, K., Lawrence, C.R., Harden, J.W. (2018): A sequential selective dissolution method to quantify storage and stability of organic carbon associated with Al and Fe hydroxide phases. Geoderma 312, 24–35. https://doi.org/10.1016/j.geoderma.2017.09.043

Heitkamp, F., Wendland, M., Offenberger, K., Gerold, G. (2012): Implications of input estimation, residue quality and carbon saturation on the predictive power of the Rothamsted Carbon Model. Geoderma 170, 168–175. https://doi.org/10.1016/j.geoderma.2011.11.005

Herrmann, A.M., Ritz, K., Nunan, N., Clode, P.L., Pett-Ridge, J., Kilburn, M.R., Murphy, D.V., O'Donnell, A.G., Stockdale, E.A. (2007): Nano-scale secondary ion mass spectrometry — A new analytical tool in biogeochemistry and soil ecology: A review article. Soil Biology and Biochemistry 39, 1835–1850. https://doi.org/10.1016/j.soilbio.2007.03.011

Horn, R., Peth, S. (2012): Mechanics of Unsaturated Soils for Agricultural Applications, in: Huang, P.M., Li, Y., Summer, M.E. (Eds.), Handbook of Soil Sciences. CRC Press, pp. 1–30.

Inagaki, T.M., Possinger, A.R., Grant, K.E., Schweizer, S.A., Mueller, C.W., Derry, L.A., Lehmann, J., Kögel-Knabner, I. (2020): Subsoil organo-mineral associations under contrasting climate conditions. Geochimica et Cosmochimica Acta 270, 244–263. https://doi.org/10.1016/j.gca.2019.11.030

ISO 9276-1:1998. Representation of results of particle size analysis -- Part 1: Graphical representation (1998).

Jastrow, J.D., Boutton, T.W., Miller, R.M. (1996): Carbon dynamics of aggregate-associated organic matter estimated by carbon-13 natural abundance. Soil Science Society of America Journal 60, 801–807.

Jensen, J.L., Schjønning, P., Watts, C.W., Christensen, B.T., Peltre, C., Munkholm, L.J. (2019): Relating soil C and organic matter fractions to soil structural stability. Geoderma 337, 834–843. https://doi.org/10.1016/j.geoderma.2018.10.034

Kahle, M., Kleber, M., Jahn, R. (2002a): Carbon storage in loess derived surface soils from Central Germany: Influence of mineral phase variables. Journal of Plant Nutrition and Soil Science 165, 141–149.

Kahle, M., Kleber, M., Jahn, R. (2002b): Predicting carbon content in illitic clay fractions from surface area, cation exchange capacity and dithionite-extractable iron. European Journal of Soil Science 53, 639–644. https://doi.org/10.1046/j.1365-2389.2002.00487.x

Kahle, M., Kleber, M., Torn, M.S., Jahn, R. (2003): Carbon Storage in Coarse and Fine Clay Fractions of Illitic Soils. Soil Science Society of America Journal 67, 1732–1739. https://doi.org/10.2136/sssaj2003.1732

Kaiser, K., Guggenberger, G. (2007): Sorptive stabilization of organic matter by microporous goethite: Sorption into small pores vs. surface complexation. European Journal of Soil Science 58, 45–59. https://doi.org/10.1111/j.1365-2389.2006.00799.x

Kaiser, K., Guggenberger, G. (2003): Mineral surfaces and soil organic matter. European Journal of Soil Science 54, 219–236. https://doi.org/10.1046/j.1365-2389.2003.00544.x

Kaiser, K., Guggenberger, G. (2000): The role of DOM sorption to mineral surfaces in the preservation of organic matter in soils. Organic Geochemistry 31, 711–725. https://doi.org/10.1016/S0146-6380(00)00046-2

Kaiser, M., Berhe, A.A. (2014): How does sonication affect the mineral and organic constituents of soil aggregates? - A review. Journal of Plant Nutrition and Soil Science 177, 479–495. https://doi.org/10.1002/jpln.201300339

Kallenbach, C.M., Frey, S.D., Grandy, A.S. (2016): Direct evidence for microbial-derived soil organic matter formation and its ecophysiological controls. Nature Communications 7. https://doi.org/10.1038/ncomms13630

Kay, B.D. (1998): Soil structure and organic carbon: A review, in: Lal, R., Kimble, J.M., Follett, R.F., Stewart, B.A. (Eds.), Soil Processes and the Carbon Cycle. CRC Press, Boca Raton, pp. 169–197. https://doi.org/10.1201/9780203739273

Kay, B.D., Dexter, A.R. (1992): The influence of dispersible clay and wetting/drying cycles on the tensile strength of a red-brown earth. Soil Research 30, 297–310. https://doi.org/10.1071/sr9920297

Kayser, G., Graf-Rosenfellner, M., Schack-Kirchner, H., Lang, F. (2019): Dynamic imaging provides novel insight into the shape and stability of soil aggregates. European Journal of Soil Science 70, 454–465. https://doi.org/doi:10.1111/ejss.12796

Keil, R.G., Tsamakis, E., Fuh, C.B., Giddings, J.C., Hedges, J.I. (1994): Mineralogical and textural controls on the organic composition of coastal marine sediments: Hydrodynamic separation using SPLITT-fractionation. Geochimica et Cosmochimica Acta 58, 879–893. https://doi.org/10.1016/0016-7037(94)90512-6

Kemper, W.D., Chepil, W.S. (1965): Size distribution of aggregates, in: Black, C.A. (Ed.), Methods of Soil Analysis: Part 1. Agronomy. pp. 499–510.

Kemper, W.D., Koch, E.J. (1966): Aggregate stability of soils from western United Sates and Canada; measurement procedure, correlations with soil constituents, in: Technical Bulletin No. 1355. Agricultural Research Service, U.S. Dept. of Agriculture, Washington, p. 52.

Kleber, M., Eusterhues, K., Keiluweit, M., Mikutta, C., Mikutta, R., Nico, P.S. (2015): Mineral–Organic Associations: Formation, Properties, and Relevance in Soil Environments. Advances in Agronomy 130, 1–140. https://doi.org/10.1016/bs.agron.2014.10.005

Kleber, M., Sollins, P., Sutton, R. (2007): A conceptual model of organo-mineral interactions in soils: self-assembly of organic molecular fragments into zonal structures on mineral surfaces. Biogeochemistry 85, 9–24. https://doi.org/10.1007/s10533-007-9103-5

Knicker, H., González-Vila, F.J., Polvillo, O., González, J.A., Almendros, G. (2005): Fire-induced transformation of C- and N- forms in different organic soil fractions from a Dystric Cambisol under a Mediterranean pine forest (Pinus pinaster). Soil Biology and Biochemistry 37, 701–718. https://doi.org/10.1016/j.soilbio.2004.09.008

Kölbl, A., Kögel-Knabner, I. (2004): Content and composition of free and occluded particulate organic matter in a differently textured arable Cambisol as revealed by solid-state 13C NMR spectroscopy. Journal of Plant Nutrition and Soil Science 167, 45–53. https://doi.org/10.1002/jpln.200321185

Kölbl, A., Schweizer, S.A., Mueller, C.W., Höschen, C., Said-Pullicino, D., Romani, M., Lugmeier, J., Schlüter, S., Kögel-Knabner, I. (2017): Legacy of Rice Roots as Encoded in Distinctive Microsites of Oxides, Silicates, and Organic Matter. Soils 1, 2.

Konert, M., Vandenberghe, J.E.F. (1997): Comparison of laser grain size analysis with pipette and sieve analysis: a solution for the underestimation of the clay fraction. Sedimentology 44, 523–535. https://doi.org/10.1046/j.1365-3091.1997.d01-38.x

Kopittke, P.M., Dalal, R.C., Hoeschen, C., Li, C., Menzies, N.W., Mueller, C.W. (2020): Soil organic matter is stabilized by organo-mineral associations through two key processes: The role of the carbon to nitrogen ratio. Geoderma 357, 113974. https://doi.org/10.1016/j.geoderma.2019.113974

Kopittke, P.M., Hernandez-Soriano, M.C., Dalal, R.C., Finn, D., Menzies, N.W., Hoeschen, C., Mueller, C.W. (2018): Nitrogen-rich microbial products provide new organo-mineral associations for the stabilization of soil organic matter. Glob Chang Biol 24, 1762–1770. https://doi.org/10.1111/gcb.14009

Kopittke, P.M., Menzies, N.W., Wang, P., McKenna, B.A., Lombi, E. (2019): Soil and the intensification of agriculture for global food security. Environment International 132, 105078. https://doi.org/10.1016/j.envint.2019.105078

Krause, L., Biesgen, D., Treder, A., Schweizer, S.A., Klumpp, E., Knief, C., Siebers, N. (2019): Initial microaggregate formation: Association of microorganisms to montmorillonite-goethite aggregates under wetting and drying cycles. Geoderma 351, 250–260. https://doi.org/10.1016/j.geoderma.2019.05.001

Krause, L., Rodionov, A., Schweizer, S.A., Siebers, N., Lehndorff, E., Klumpp, E., Amelung, W. (2018): Microaggregate stability and storage of organic carbon is affected by clay content in arable Luvisols. Soil and Tillage Research 182, 123–129.

Kristiansen, S.M., Schjønning, P., Thomsen, I.K., Olesen, J.E., Kristensen, K., Christensen, B.T. (2006): Similarity of differently sized macro-aggregates in arable soils of different texture. Geoderma 137, 147–154. https://doi.org/10.1016/j.geoderma.2006.08.005

Laird, D. (2001): Nature of clay-humic complexes in an agricultural soil: II. Scanning electron microscopy analysis. Soil Science Society of America Journal 65, 1419–1425.

Lal, R. (2018): Digging deeper: A holistic perspective of factors affecting soil organic carbon sequestration in agroecosystems. Global Change Biology 24, 3285–3301. https://doi.org/10.1111/gcb.14054

Lavallee, J.M., Soong, J.L., Cotrufo, M.F. (2019): Conceptualizing soil organic matter into particulate and mineral-associated forms to address global change in the 21st century. Global Change Biology 0, 1–13. https://doi.org/10.1111/gcb.14859

Le Bissonnais, Y. (1996): Aggregate stability and assessment of soil crustability and erodibility: I. Theory and methodology. Stabilite structurale et evaluation de la sensibilite des sols a la battance et a l'erosion: I: Theorie et methologie 47, 425–437.

Lobe, I., Sandhage-Hofmann, A., Brodowski, S., Preez, C.C. du, Amelung, W. (2011): Aggregate dynamics and associated soil organic matter content as influenced by prolonged arable cropping in the South African Highveld. Geoderma 162, 251–259.

Loisel, J., Casellas Connors, J.P., Hugelius, G., Harden, J.W., Morgan, C.L. (2019): Soils can help mitigate CO_2 emissions, despite the challenges. Proceedings of the National Academy of Sciences 116, 10211–10212. https://doi.org/10.1073/pnas.1900444116

Maarastawi, S.A., Frindte, K., Linnartz, M., Knief, C. (2018): Crop Rotation and Straw Application Impact Microbial Communities in Italian and Philippine Soils and the Rhizosphere of Zea mays. Frontiers in Microbiology 9, 1295. https://doi.org/10.3389/fmicb.2018.01295

Macht, F., Eusterhues, K., Pronk, G.J., Totsche, K.U. (2011): Specific surface area of clay minerals: Comparison between atomic force microscopy measurements and bulk-gas (N2) and -liquid (EGME) adsorption methods. Applied Clay Science 53, 20–26. https://doi.org/10.1016/j.clay.2011.04.006

Manzoni, S., Taylor, P., Richter, A., Porporato, A., Ågren, G.I. (2012): Environmental and stoichiometric controls on microbial carbon-use efficiency in soils. New Phytologist 196, 79–91. https://doi.org/10.1111/j.1469-8137.2012.04225.x

Mayer, A., Hausfather, Z., Jones, A.D., Silver, W.L. (2018): The potential of agricultural land management to contribute to lower global surface temperatures. Science Advances 4, eaaq0932. https://doi.org/10.1126/sciadv.aaq0932

Mayer, L.M. (1999): Extent of coverage of mineral surfaces by organic matter in marine sediments. Geochimica et Cosmochimica Acta 63, 207–215. http://dx.doi.org/10.1016/S0016-7037(99)00028-9

Mayer, L.M. (1994): Relationships between mineral surfaces and organic carbon concentrations in soils and sediments. Chemical Geology 114, 347–363. https://doi.org/10.1016/0009-2541(94)90063-9

Mayer, L.M., Xing, B. (2001): Organic Matter–Surface Area Relationships in Acid Soils. Soil Science Society of America Journal 65, 250–258. https://doi.org/10.2136/sssaj2001.651250x

Mayes, M., Jagadamma, S., Ambaye, H., Petridis, L., Lauter, V. (2013): Neutron reflectometry reveals the internal structure of organic compounds deposited on aluminum oxide. Geoderma 192, 182–188. https://doi.org/10.1016/j.geoderma.2012.07.025

McCarthy, J.F., Ilavsky, J., Jastrow, J.D., Mayer, L.M., Perfect, E., Zhuang, J. (2008): Protection of organic carbon in soil microaggregates via restructuring of aggregate porosity and filling of pores with accumulating organic matter. Geochimica et Cosmochimica Acta 72, 4725–4744. https://doi.org/10.1016/j.gca.2008.06.015

Mehra, O.P., Jackson, M.L. (1958): Iron Oxide Removal from Soils and Clays by a Dithionite-Citrate System Buffered with Sodium Bicarbonate. Clays and Clay Minerals 7, 317–327. https://doi.org/10.1346/ccmn.1958.0070122

Mikutta, R., Kleber, M., Kaiser, K., Jahn, R. (2005): Review: Organic Matter Removal from Soils using Hydrogen Peroxide, Sodium Hypochlorite, and Disodium Peroxodisulfate. Soil Science Society of America Journal 69, 120–135.

Mikutta, R., Turner, S., Schippers, A., Gentsch, N., Meyer-Stüve, S., Condron, L.M., Peltzer, D.A., Richardson, S.J., Eger, A., Hempel, G., Kaiser, K., Klotzbücher, T., Guggenberger, G. (2019): Microbial and abiotic controls on mineral-associated organic matter in soil profiles along an ecosystem gradient. Scientific Reports 9, 10294. https://doi.org/10.1038/s41598-019-46501-4

Miller, R.M., Jastrow, J.D. (1990): Hierarchy of root and mycorrhizal fungal interactions with soil aggregation. Soil Biology and Biochemistry 22, 579–584.

Mitchell, P., Simpson, A., Soong, R., Simpson, M. (2018): Nuclear Magnetic Resonance Analysis of Changes in Dissolved Organic Matter Composition with Successive Layering on Clay Mineral Surfaces. Soil Systems 2, 8. https://doi.org/10.3390/soils2010008

Moni, C., Derrien, D., Hatton, P.-J., Zeller, B., Kleber, M. (2012): Density fractions versus size separates: does physical fractionation isolate functional soil compartments? Biogeosciences 9, 5181–5197. https://doi.org/10.5194/bg-9-5181-2012

Moon, J., Xia, K., Williams, M.A. (2019): Consistent proteinaceous organic matter partitioning into mineral and organic soil fractions during pedogenesis in diverse ecosystems. Biogeochemistry 142, 117–135. https://doi.org/10.1007/s10533-018-0523-1

Mueller, C.W., Weber, P.K., Kilburn, M.R., Hoeschen, C., Kleber, M., Pett-Ridge, J. (2013): Advances in the Analysis of Biogeochemical Interfaces: NanoSIMS to Investigate Soil Microenvironments. Advances in Agronomy 121, 1–46. https://doi.org/10.1016/b978-0-12-407685-3.00001-3

Murer, E.J., Baumgarten, A., Eder, G., Gerzabek, M.H., Kandeler, E., Rampazzo, N. (1993): An improved sieving machine for estimation of soil aggregate stability (SAS). Geoderma 56, 539–547. https://doi.org/10.1016/0016-7061(93)90133-6

Oades, J.M. (1988): The retention of organic matter in soils. Biogeochemistry 5, 35–70.

Oades, J.M. (1984): Soil organic matter and structural stability: mechanisms and implications for management. Plant and Soil 76, 319–337.

Oades, J.M., Waters, A.G. (1991): Aggregate hierarchy in soils. Soil Research 29, 815–828. http://dx.doi.org/10.1071/SR9910815

Obalum, S.E., Uteau-Puschmann, D., Peth, S. (2019): Reduced tillage and compost effects on soil aggregate stability of a silt-loam Luvisol using different aggregate stability tests. Soil and Tillage Research 189, 217–228. https://doi.org/10.1016/j.still.2019.02.002

Ollivier, J., Töwe, S., Bannert, A., Hai, B., Kastl, E.-M., Meyer, A., Su, M.X., Kleineidam, K., Schloter, M. (2011): Nitrogen turnover in soil and global change. FEMS Microbiology Ecology 78, 3–16. https://doi.org/10.1111/j.1574-6941.2011.01165.x

Ouberai, M.M., Xu, K., Welland, M.E. (2014): Effect of the interplay between protein and surface on the properties of adsorbed protein layers. Biomaterials 35, 6157–6163. https://doi.org/10.1016/j.biomaterials.2014.04.012

Paradiś, A., Brueck, C., Meisenheimer, D., Wanzek, T., Dragila, M.I. (2017): Sandy Soil Microaggregates: Rethinking Our Understanding of Hydraulic Function. Vadose Zone Journal 16. https://doi.org/10.2136/vzj2017.05.0090

Paustian, K., Lehmann, J., Ogle, S., Reay, D., Robertson, G.P., Smith, P. (2016): Climate-smart soils. Nature 532, 49. https://doi.org/10.1038/nature17174

Paustian, K., Parton, W.J., Persson, J. (1992): Modeling Soil Organic Matter in Organic-Amended and Nitrogen-Fertilized Long-Term Plots. Soil Science Society of America Journal 56, 476. https://doi.org/10.2136/sssaj1992.03615995005600020023x

Petridis, L., Ambaye, H., Jagadamma, S., Kilbey, S.M., Lokitz, B.S., Lauter, V., Mayes, M.A. (2014): Spatial Arrangement of Organic Compounds on a Model Mineral Surface: Implications for Soil Organic Matter Stabilization. Environmental Science & Technology 48, 79–84. https://doi.org/10.1021/es403430k

Pronk, G.J., Heister, K., Kögel-Knabner, I. (2013): Is turnover and development of organic matter controlled by mineral composition? Soil Biology and Biochemistry 67, 235–244. https://doi.org/10.1016/j.soilbio.2013.09.006

Pronk, G.J., Heister, K., Vogel, C., Babin, D., Bachmann, J., Ding, G.-C., Ditterich, F., Gerzabek, M.H., Giebler, J., Hemkemeyer, M., Kandeler, E., Kunhi Mouvenchery, Y., Miltner, A., Poll, C., Schaumann, G.E., Smalla, K., Steinbach, A., Tanuwidjaja, I., Tebbe, C.C., Wick, L.Y., Woche, S.K., Totsche, K.U., Schloter, M., Kögel-Knabner, I. (2017): Interaction of minerals, organic matter, and microorganisms during biogeochemical interface formation as shown by a series of artificial soil experiments. Biology and Fertility of Soils 53, 9–22. https://doi.org/10.1007/s00374-016-1161-1

Pronk, G.J., Katja Heister, Ding, G.-C., Smalla, K., Kögel-Knabner, I. (2012): Development of biogeochemical interfaces in an artificial soil incubation experiment; aggregation and formation of organo-mineral associations. Geoderma 189–190, 585–594. https://doi.org/10.1016/j.geoderma.2012.05.020

Puget, P., Chenu, C., Balesdent, J. (2000): Dynamics of soil organic matter associated with particle-size fractions of water-stable aggregates. European Journal of Soil Science 51, 595–605. https://doi.org/doi:10.1111/j.1365-2389.2000.00353.x

Rabbi, S.M.F., Minasny, B., McBratney, A.B., Young, I.M. (2020): Microbial processing of organic matter drives stability and pore geometry of soil aggregates. Geoderma 360, 114033. https://doi.org/10.1016/j.geoderma.2019.114033

Raine, S.R., So, H.B. (1994): Ultrasonic Dispersion of Soil in Water: the Effect of Suspension Properties on Energy Dissipation and Soil Dispersion. Australian Journal of Soil Research 32, 1157–1174.

Ransom, B., Bennett, R.H., Baerwald, R., Shea, K. (1997): TEM study of in situ organic matter on continental margins: Occurrence and the "monolayer" hypothesis. Marine Geology 138, 1–9. https://doi.org/10.1016/S0025-3227(97)00012-1

Rasmussen, C., Heckman, K., Wieder, W.R., Keiluweit, M., Lawrence, C.R., Berhe, A.A., Blankinship, J.C., Crow, S.E., Druhan, J.L., Hicks Pries, C.E., Marin-Spiotta, E., Plante, A.F., Schädel, C., Schimel, J.P., Sierra, C.A., Thompson, A., Wagai, R. (2018): Beyond clay: towards an improved set of variables for predicting soil organic matter content. Biogeochemistry 137, 297–306. https://doi.org/10.1007/s10533-018-0424-3

Remusat, L., Hatton, P.J., Nico, P.S., Zeller, B., Kleber, M., Derrien, D. (2012): NanoSIMS study of organic matter associated with soil aggregates: advantages, limitations, and combination with STXM. Environmental Science & Technology 46, 3943–9. https://doi.org/10.1021/es203745k

Renard, P., Allard, D. (2013): Connectivity metrics for subsurface flow and transport. Advances in Water Resources 51, 168–196. https://doi.org/10.1016/j.advwatres.2011.12.001

Rennert, T., Totsche, K.U., Heister, K., Kersten, M., Thieme, J. (2012): Advanced spectroscopic, microscopic, and tomographic characterization techniques to study biogeochemical interfaces in soil. Journal of Soils and Sediments 12, 3–23. https://doi.org/10.1007/s11368-011-0417-5

RStudio Team (2015): RStudio: Integrated Development Environment for R. RStudio, Inc., Boston, USA.

Sanderman, J., Hengl, T., Fiske, G.J. (2017): Soil carbon debt of 12,000 years of human land use. Proceedings of the National Academy of Sciences 114, 9575. https://doi.org/10.1073/pnas.1706103114

Scharlemann, J.P.W., Tanner, E.V.J., Hiederer, R., Kapos, V. (2014): Global soil carbon: understanding and managing the largest terrestrial carbon pool. Carbon Management 5, 81–91. https://doi.org/10.4155/cmt.13.77

Schindelin, J., Rueden, C.T., Hiner, M.C., Eliceiri, K.W. (2015): The ImageJ ecosystem: An open platform for biomedical image analysis. Molecular Reproduction and Development 82, 518–529. https://doi.org/10.1002/mrd.22489

Schjønning, P., de Jonge, L.W., Munkholm, L.J., Moldrup, P., Christensen, B.T., Olesen, J.E. (2012): Clay Dispersibility and Soil Friability—Testing the Soil Clay-to-Carbon Saturation Concept. Vadose Zone Journal 11, 0. https://doi.org/10.2136/vzj2011.0067

Schlesinger, W.H., Amundson, R. (2019): Managing for soil carbon sequestration: Let's get realistic. Global Change Biology 25, 386–389. https://doi.org/10.1111/gcb.14478

Schlüter, S., Sheppard, A., Brown, K., Wildenschild, D. (2014): Image processing of multiphase images obtained via X-ray microtomography: A review. Water Resources Research 50, 3615–3639. https://doi.org/10.1002/2014WR015256

Schmidt, M.W.I., Torn, M.S., Abiven, S., Dittmar, T., Guggenberger, G., Janssens, I.A., Kleber, M., Kögel-Knabner, I., Lehmann, J., Manning, D.A.C., Nannipieri, P., Rasse, D.P., Weiner, S., Trumbore, S.E. (2011): Persistence of soil organic matter as an ecosystem property. Nature 478, 49–56. https://doi.org/10.1038/nature10386

Schröder, P., Huber, B., Olazábal, U., Kämmerer, A., Munch, J.C. (2002): Land use and sustainability: FAM Research Network on Agroecosystems. Geoderma 105, 155–166. https://doi.org/10.1016/S0016-7061(01)00101-X

Schrumpf, M., Kaiser, K., Guggenberger, G., Persson, T., Kögel-Knabner, I., Schulze, E.D. (2013): Storage and stability of organic carbon in soils as related to depth, occlusion within aggregates, and attachment to minerals. Biogeosciences 10, 1675–1691. https://doi.org/10.5194/bg-10-1675-2013

Schulz, S., Brankatschk, R., Dümig, A., Kögel-Knabner, I., Schloter, M., Zeyer, J. (2013): The role of microorganisms at different stages of ecosystem development for soil formation. Biogeosciences 10, 3983–3996. https://doi.org/10.5194/bg-10-3983-2013

Schumaker, N.H. (1996): Using landscape indices to predict habitat connectivity. Ecology 77, 1210–1225.

Schwertmann, U. (1964): Differenzierung der Eisenoxide des Bodens durch Extraktion mit Ammoniumoxalat-Lösung. Journal of Plant Nutrition and Soil Science 105, 194–202. https://doi.org/10.1002/jpln.3591050303

Segoli, M., De Gryze, S., Dou, F., Lee, J., Post, W.M., Denef, K., Six, J. (2013): AggModel: A soil organic matter model with measurable pools for use in incubation studies. Ecological Modelling 263, 1–9. https://doi.org/10.1016/j.ecolmodel.2013.04.010

Six, J., Bossuyt, H., Degryze, S., Denef, K. (2004): A history of research on the link between (micro)aggregates, soil biota, and soil organic matter dynamics. Soil and Tillage Research 79, 7–31.

Six, J., Callewaert, P., Lenders, S., De Gryz, S., Morris, S.J., Gregorich, E.G., Paul, E.A., Paustian, K. (2002): Measuring and understanding carbon storage in afforested soils by physical fractionation. Soil Science Society of America Journal 66, 1981–1987.

Six, J., Elliott, E.T., Paustian, K., Doran, J.W. (1998): Aggregation and soil organic matter accumulation in cultivated and native grassland soils. Soil Science Society of America Journal 62, 1367–1377.

Six, J., Paustian, K., Elliott, E.T., Combrink, C. (2000): Soil structure and organic matter I. Distribution of aggregate-size classes and aggregate-associated carbon. Soil Science Society of America Journal 64, 681–689. https://doi.org/10.2136/sssaj2000.642681x

Skidmore, E.L., Powers, D.H. (1982): Dry soil-aggregate stability: energy-based index. Soil Science Society of America Journal 46, 1274–1279.

Smith, P., House, J.I., Bustamante, M., Sobocká, J., Harper, R., Pan, G., West, P.C., Clark, J.M., Adhya, T., Rumpel, C., Paustian, K., Kuikman, P., Cotrufo, M.F., Elliott, J.A., McDowell, R., Griffiths, R.I., Asakawa, S., Bondeau, A., Jain, A.K., Meersmans, J., Pugh, T.A.M. (2016): Global change pressures on soils from land use and management. Global Change Biology 22, 1008–1028. https://doi.org/10.1111/gcb.13068

Sollins, P., Kramer, M.G., Swanston, C., Lajtha, K., Filley, T., Aufdenkampe, A.K., Wagai, R., Bowden, R.D. (2009): Sequential density fractionation across soils of contrasting mineralogy: evidence for both microbial- and mineral-controlled soil organic matter stabilization. Biogeochemistry 96, 209–231. https://doi.org/10.1007/s10533-009-9359-z

Sollins, P., Swanston, C., Kleber, M., Filley, T., Kramer, M., Crow, S., Caldwell, B.A., Lajtha, K., Bowden, R. (2006): Organic C and N stabilization in a forest soil: Evidence from sequential density fractionation. Soil Biology and Biochemistry 38, 3313–3324. https://doi.org/10.1016/j.soilbio.2006.04.014

Sommer, C., Strähle, C., Köthe, U., Hamprecht, F.A. (2011): ilastik: Interactive Learning and Segmentation Toolkit. Presented at the Eighth IEEE International Symposium on Biomedical Imaging (ISBI), pp. 230–233.

Sommer, M., Wehrhan, M., Zipprich, M., Weller, U., Zu Castell, W., Ehrich, S., Tandler, B., Selige, T. (2003): Hierarchical data fusion for mapping soil units at field scale. Geoderma 112, 179–196. https://doi.org/10.1016/S0016-7061(02)00305-1

Souza, I., Almeida, L.F., L. Jesus, G., Kleber, M., Silva, I.R. (2017): The mechanisms of organic carbon protection and dynamics of C-saturation in Oxisols vary with particle-size distribution. European Journal of Soil Science 68, 726–739. https://doi.org/10.1111/ejss.12463

Steffens, M., Rogge, D.M., Mueller, C.W., Höschen, C., Lugmeier, J., Kölbl, A., Kögel-Knabner, I. (2017): Identification of Distinct Functional Microstructural Domains Controlling C Storage in Soil. Environmental Science & Technology 51, 12182–12189. https://doi.org/10.1021/acs.est.7b03715

Stewart, C.E., Paustian, K., Conant, R.T., Plante, A.F., Six, J. (2008): Soil carbon saturation: Evaluation and corroboration by long-term incubations. Soil Biology and Biochemistry 40, 1741–1750. https://doi.org/10.1016/j.soilbio.2008.02.014

Stewart, C.E., Paustian, K., Conant, R.T., Plante, A.F., Six, J. (2007): Soil carbon saturation: concept, evidence and evaluation. Biogeochemistry 86, 19–31. https://doi.org/10.1007/s10533-007-9140-0

Sulman, B.N., Moore, J.A.M., Abramoff, R., Averill, C., Kivlin, S., Georgiou, K., Sridhar, B., Hartman, M.D., Wang, G., Wieder, W.R., Bradford, M.A., Luo, Y., Mayes, M.A., Morrison, E., Riley, W.J., Salazar, A., Schimel, J.P., Tang, J., Classen, A.T. (2018): Multiple models and experiments underscore large uncertainty in soil carbon dynamics. Biogeochemistry 141, 109–123. https://doi.org/10.1007/s10533-018-0509-z

Theng, B.K.G., Ristori, G.G., Santi, C.A., Percival, H.J. (1999): An improved method for determining the specific surface areas of topsoils with varied organic matter content, texture and clay mineral composition. European Journal of Soil Science 50, 309–316. https://doi.org/10.1046/j.1365-2389.1999.00230.x

Tisdall, J.M. (1994): Possible role of soil microorganisms in aggregation in soils. Plant and Soil 159, 115–121.

Tisdall, J.M., Oades, J.M. (1982): Organic matter and water-stable aggregates in soils. Journal of Soil Science 33, 141–163.

Torn, M.S., Trumbore, S.E., Chadwick, O.A., Vitousek, P.M., Hendricks, D.M. (1997): Mineral control of soil organic carbon storage and turnover. Nature 389, 170–173.

Totsche, K.U., Amelung, W., Gerzabek, M.H., Guggenberger, G., Klumpp, E., Knief, C., Lehndorff, E., Mikutta, R., Peth, S., Prechtel, A., Ray, N., Kögel-Knabner, I. (2018): Microaggregates in soils. Journal of Plant Nutrition and Soil Science 181, 104–136.

Trivedi, P., Delgado-Baquerizo, M., Jeffries, T.C., Trivedi, C., Anderson, I.C., Lai, K., McNee, M., Flower, K., Pal Singh, B., Minkey, D., Singh, B.K. (2017): Soil aggregation and associated microbial

communities modify the impact of agricultural management on carbon content. Environmental Microbiology 19, 3070–3086. https://doi.org/10.1111/1462-2920.13779

Tscherko, D., Hammesfahr, U., Marx, M.-C., Kandeler, E. (2004): Shifts in rhizosphere microbial communities and enzyme activity of Poa alpina across an alpine chronosequence. Soil Biology and Biochemistry 36, 1685–1698. https://doi.org/10.1016/j.soilbio.2004.07.004

Vaughan, E., Matos, M., Ríos, S., Santiago, C., Marín-Spiotta, E. (2019): Clay and climate are poor predictors of regional-scale soil carbon storage in the US Caribbean. Geoderma 354, 113841. https://doi.org/10.1016/j.geoderma.2019.06.044

Virto, I., Barré, P., Chenu, C. (2008): Microaggregation and organic matter storage at the silt-size scale. Geoderma 146, 326–335. https://doi.org/10.1016/j.geoderma.2008.05.021

Virto, I., Moni, C., Swanston, C., Chenu, C. (2010): Turnover of intra- and extra-aggregate organic matter at the silt-size scale. Geoderma 156, 1–10. https://doi.org/10.1016/j.geoderma.2009.12.028

Vogel, C., Heister, K., Buegger, F., Tanuwidjaja, I., Haug, S., Schloter, M., Kögel-Knabner, I. (2015): Clay mineral composition modifies decomposition and sequestration of organic carbon and nitrogen in fine soil fractions. Biology and Fertility of Soils 51, 427–442. https://doi.org/10.1007/s00374-014-0987-7

Vogel, C., Mueller, C.W., Hoschen, C., Buegger, F., Heister, K., Schulz, S., Schloter, M., Kogel-Knabner, I. (2014): Submicron structures provide preferential spots for carbon and nitrogen sequestration in soils. Nature Communications 5, 2947. https://doi.org/10.1038/ncomms3947

Wagai, R., Kajiura, M., Uchida, M., Asano, M. (2018): Distinctive Roles of Two Aggregate Binding Agents in Allophanic Andisols: Young Carbon and Poorly-Crystalline Metal Phases with Old Carbon. Soil Systems 2, 29. https://doi.org/10.3390/soilsystems2020029

Wagai, R., Mayer, L.M., Kitayama, K. (2009): Extent and nature of organic coverage of soil mineral surfaces assessed by a gas sorption approach. Geoderma 149, 152–160. https://doi.org/10.1016/j.geoderma.2008.11.032

Watteau, F., Villemin, G., Bartoli, F., Schwartz, C., Morel, J.L. (2012): 0–20 µm aggregate typology based on the nature of aggregative organic materials in a cultivated silty topsoil. Soil Biology and Biochemistry 46, 103–114. https://doi.org/10.1016/j.soilbio.2011.11.021

Wattel-Koekkoek, E.J.W., Van Genuchten, P.P.L., Buurman, P., Van Lagen, B. (2001): Amount and composition of clay-associated soil organic matter in a range of kaolinitic and smectitic soils. Geoderma 99, 27–49. https://doi.org/10.1016/S0016-7061(00)00062-8

Webster, R., Lark, R.M. (2013): Nested sampling and analysis, In: Field Sampling for Environmental Science and Management. Routledge, London, UK.

Wiesmeier, M., Urbanski, L., Hobley, E., Lang, B., von Lützow, M., Marin-Spiotta, E., van Wesemael, B., Rabot, E., Ließ, M., Garcia-Franco, N., Wollschläger, U., Vogel, H.J., Kögel-Knabner, I. (2019): Soil organic carbon storage as a key function of soils - A review of drivers and indicators at various scales. Geoderma 333, 149–162. https://doi.org/10.1016/j.geoderma.2018.07.026

Wiseman, C.L.S., Püttmann, W. (2005): Soil organic carbon and its sorptive preservation in central Germany. European Journal of Soil Science 56, 65–76. https://doi.org/10.1111/j.1351-0754.2004.00655.x

Wollny, E. (1898): Untersuchungen über den Einfluß der mechanischen Bearbeitung auf die Fruchtbarkeit des Bodens. Forschungen auf dem Gebiete der Agrikultur Physik 20, 23–290.

Yang, X.M., Drury, C.F., Reynolds, W.D., Yang, J.Y. (2016): How do changes in bulk soil organic carbon content affect carbon concentrations in individual soil particle fractions? Scientific Reports 6. https://doi.org/10.1038/srep27173

Yeasmin, S., Singh, B., Johnston, C.T., Sparks, D.L. (2017): Organic carbon characteristics in density fractions of soils with contrasting mineralogies. Geochimica et Cosmochimica Acta 218, 215–236. https://doi.org/10.1016/j.gca.2017.09.007

Zhao, L., Sun, Y., Zhang, X., Yang, X., Drury, C.F. (2006): Soil organic carbon in clay and silt sized particles in Chinese mollisols: Relationship to the predicted capacity. Geoderma 132, 315–323. https://doi.org/10.1016/j.geoderma.2005.04.026

Zumsteg, A., Luster, J., Göransson, H., Smittenberg, R.H., Brunner, I., Bernasconi, S.M., Zeyer, J., Frey, B. (2012): Bacterial, Archaeal and Fungal Succession in the Forefield of a Receding Glacier. Microbial Ecology 63, 552–564. https://doi.org/10.1007/s00248-011-9991-8

6 Acknowledgments

I would like to thank the many people who have contributed to this thesis.

First of all, thanks to my supervisor Prof. Kögel-Knabner for entrusting me this journey into the microworld of soil aggregates thanks to her initial conception of this project. I am deeply indebted to her concerted effort, inspiration and good spirit during intensive scientific discussions. A special thanks also to Christian Schurig for the introduction to Freising during the first months. Throughout the recent years, I am especially grateful for the considerable degrees of freedom I have been allowed in order to pursue the research directions I found most exciting.

I have had the fortune of great co-authors and colleagues. I thank all my co-authors for their helpful comments, patience and support. Especially the intensive exchange of ideas with Carsten Mueller, Carmen Höschen and Angelika Kölbl is acknowledged. I am also thankful to all other group members who always had an open ear for my needs and ideas, especially Markus Steffens, Peter Schad and Werner Häusler. Thanks to Luis Colocho and Jörg Prietzel for letting me assist during some exciting days of synchotron measurements. For maximizing the research output during NanoSIMS measurements the exceptional efforts of Hans Lugmeier and Gerti Harrington is greatly acknowledged. Parts of my work using density fractionation and aggregate size distribution would not have been possible without the help of Verena Schäuble, Franziska Bucka, Franziska Steiner and Sandra Bierbach. The vigorous atmosphere and the solidary spirit in the laboratory is thanks to the technicians each gifted with a special hand for analytical methods. Furthermore, I shared great breaks over lunch or coffee with my fellow PhD students which turned potential setbacks in the laboratory or peer-reviewing into enjoyable experiences. A special thanks to my optimistic and encouraging office mate, Evelin Pihlaps, during the last two years. In addition to the great lab community, many wonderful flatmates like Rebekka, Anna, Johannes and Simon have supported me with occasional distraction and unwavering encouragement throughout my scientific endeavors. It is a fortune to always have someone around to discuss ideas of soil aggregation over a beer, participate together in activities at the science-policy interface or tune the best colors for soil texture triangle stickers.

Right from the beginning, my project was set up with great collaborations under the framework of the MADSoil research unit. The Deutsche Forschungsgemeinschaft is greatly acknowledged for the financial support to establish the excellent research unit RU 2179 and our project through KO 1035/48-1. I am thankful especially to Vincent Felde, Lars Krause, Danh Biesgen and Claudia Knief for the extensive exchange and collaborative work. I am also thankful to all other collaborations that I came across and were crucial for the development of this work. I would like to thank Steffen Schlüter for the pleasant exchange at the UFZ in Halle,

the organization of a great workshop supported by the DBG and the exciting collaboration. Thanks to Markus Graf-Rosenfellner, Gilles Kayser and Friederike Lang for the hospitality at the University of Freiburg and making their dynamic image analysis equipment available for the size distribution measurements. For access and the introduction to electron microscopy, I wish to thank Beate Rockel from the Institute of Electron Microscopy of TUM in Garching and Dominik Fiedler at the Fraunhofer Institute for Process Engineering and Packaging. The intensive exchange with Rota Wagai and Peter Kopittke during their visits was very encouraging during the interpretation and writing work. Among many inspiring conferences where I could present and discuss my latest research, I would like to especially thank the German Soil Science Society (DBG) and the European Geosciences Union (EGU) for their support of workshops and events with early-career scientists.

Last but not least I'm deeply indebted to the great hospitality of a handful of Australian-based researchers who hosted me for a short visit and research stay. Thanks Peter Kopittke, Matthew Tighe, Rhiannon Smith, Brian Wilson and Yui Osanai for the 'Down Under' perspectives on soil processes and enduring me during the final stage of my thesis. Large parts of the written part of my thesis were fleshed out during my travel through Australian landscapes.

Finally, I want to thank Anna for her patience and support.

A heartful thanks everyone for the fruitful discussions and support!

Steffen Schweizer

Freising, 27th January 2020

7 Appendix

A Study I

Study I is published as follows:

Schweizer, S. A., C. Höschen, S. Schlüter, I. Kögel-Knabner, C. W. Mueller (2018): Rapid soil structure formation after glacial retreat driven by organic matter accrual at the microscale. Global Change Biology 24(4), 1637–1650. 10.1111/gcb.14014

Graphical Abstract

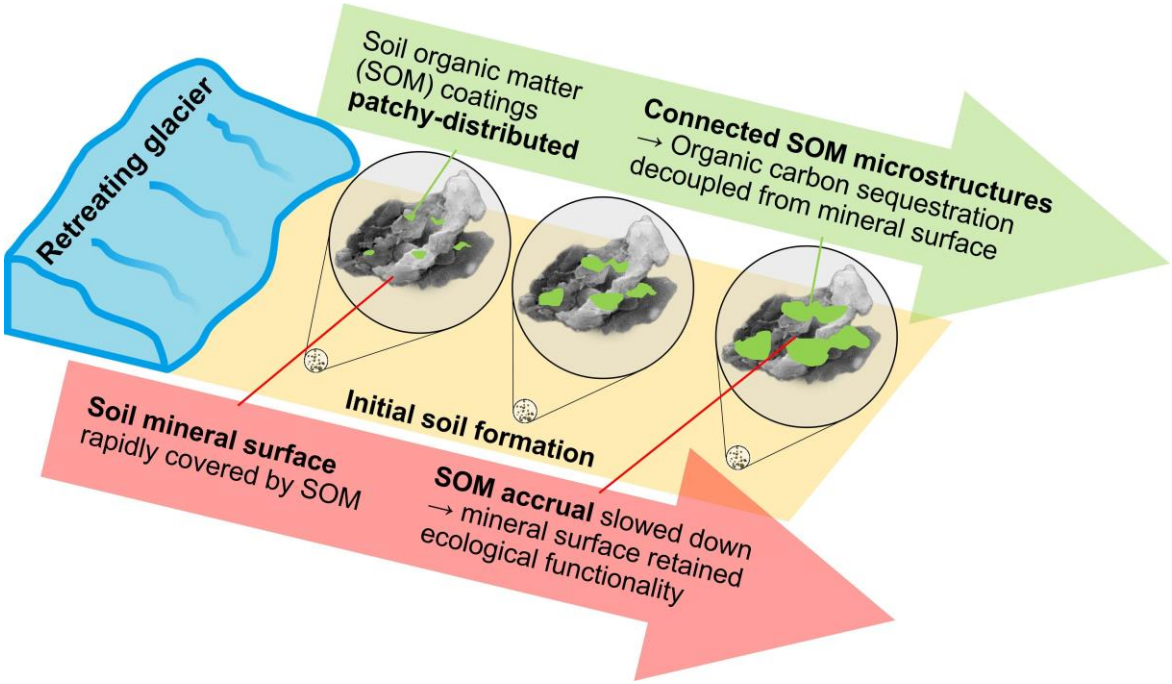

B Study II

Study II is unpublished to date (July 2020):

Schweizer, S. A., C. W. Mueller, C. Hoeschen, P. Ivanov, I. Kögel-Knabner: Mineral-associated organic matter accretion is decoupled from mineral surface area along a soil texture gradient.

C Study III

Study III is published as follows:

Schweizer, S. A., F. B. Bucka, M. Graf-Rosenfellner, I. Kögel-Knabner (2019): Soil microaggregate size composition and organic matter distribution as affected by clay content. Geoderma 355, 113901. 10.1016/j.geoderma.2019.113901

D Study IV

Study IV is published as follows:

V. J M. N L. Felde, **S. A. Schweizer**, D. Biesgen, A. Ulbrich, D. Uteau, C. Knief, M. Graf-Rosenfellner, I. Kögel-Knabner and S. Peth (2020): Wet sieving versus dry crushing: Soil microaggregates reveal different physical structure, bacterial diversity and organic matter composition in a clay gradient. European Journal of Soil Science, 1–19. 10.1111/ejss.13014

G List of scientific contributions

G.1 Peer-reviewed publications

Felde, V.J., **S. A. Schweizer**, D. Biesgen, A. Ulbrich, D. Uteau, C. Knief, M. Graf-Rosenfellner, I. Kögel-Knabner, S. Peth. (2020), Wet sieving versus dry crushing: Soil microaggregates reveal different physical structure, bacterial diversity and organic matter composition in a clay gradient. European Journal of Soil Science. 10.1111/ejss.13014

Guhra, T., K. Stolze, **S. Schweizer**, K. U. Totsche (2020): Earthworm mucus contributes to the formation of organo-mineral associations in soil. Soil Biology and Biochemistry 145, 107785. 10.1016/j.soilbio.2020.107785

Inagaki, T. M., A. R. Possinger, K. E. Grant, **S. A. Schweizer**, C. W. Mueller, L. A. Derry, J. Lehmann, I. Kögel-Knabner (2020): Subsoil Organo-Mineral Associations under Contrasting Climate Conditions. Geochimica et Cosmochimica Acta 270, 244–263. 10.1016/j.gca.2019.11.030

Schweizer, S. A., F. B. Bucka, M. Graf-Rosenfellner, I. Kögel-Knabner (2019): Soil microaggregate size composition and organic matter distribution as affected by clay content. Geoderma 355, 113901. 10.1016/j.geoderma.2019.113901

Krause, L., D. Biesgen, A. Treder, **S. A. Schweizer**, E. Klumpp, C. Knief, N. Siebers (2019): Initial microaggregate formation: Association of microorganisms to montmorillonite-goethite aggregates under wetting and drying cycles. Geoderma 351, 250–260. 10.1016/j.geoderma.2019.05.001

Schweizer, S. A., C. Höschen, S. Schlüter, I. Kögel-Knabner, C. W. Mueller (2018): Rapid soil structure formation after glacial retreat driven by organic matter accrual at the microscale. Global Change Biology 24(4), 1637–1650. 10.1111/gcb.14014

Krause, L., A. Rodionov, **S. A. Schweizer**, N. Siebers, E. Lehndorff, E. Klumpp, W. Amelung (2018): Microaggregate stability and storage of organic carbon is affected by clay content in arable Luvisols. Soil and Tillage Research 182, 123–129. 10.1016/j.still.2018.05.003

Kölbl, A., **S. A. Schweizer**, C. W. Mueller, C. Höschen, D. Said-Pullicino, M. Romani, J. Lugmeier, S. Schlüter, I. Kögel-Knabner (2017): Legacy of Rice Roots as Encoded in Distinctive Microsites of Oxides, Silicates, and Organic Matter. Soils 1(1), 2. 10.3390/soils1010002

Schweizer, S. A., B. Seitz, M. G. A. van der Heijden, R. Schulin, S. Tandy (2018): Impact of organic and conventional farming systems on wheat grain uptake and soil bioavailability of zinc and cadmium. Science of the Total Environment 639, 608–616. 10.1016/j.scitotenv.2018.05.187

Hassan, L., M.J. Reppke, N. Thieme, **S.A. Schweizer,** C. W. Mueller, J. P. Benz (2017): Comparing the physiochemical parameters of three celluloses reveals new insights into substrate suitability for fungal enzyme production. Fungal Biology and Biotechnology 4(10). 10.1186/s40694-017-0039-9

Schweizer, S. A., H. Fischer, V. Häring, K. Stahr (2017): Soil structure breakdown following land use change from forest to maize in Northwest Vietnam. Soil and Tillage Research 166, 10–17. 10.1016/j.still.2016.09.010

Gebhard, E., N. Hagemann, L. Hensler, **S. Schweizer**, Carla Wember (2015): Agriculture and Food 2050: Visions to Promote Transformation Driven by Science and Society. Journal of Agricultural and Environmental Ethics 28(3). 497–516. 10.1007/s10806-015-9532-4

Lutz, R., J. Dietrich, L. Voget-Kleschin, M. Hilscher, D. Manoharan, **S. Schweizer**, A. C. Bellows (2011): Ethics of Food and Nutrition Security oder: Kann ethische Theorie die ethische Wahrnehmungskompetenz steigern? Eine Pilotstudie zur empirischen Unterrichtsforschung. Zeitschrift für Didaktik der Philosophie und Ethik (ZDPE) 3: 43–56.

G.2 Conference presentations (only first-authored)

Schweizer, S. A., F. B. Bucka, M. Graf-Rosenfellner, I. Kögel-Knabner (2019): Soil organic matter distribution governed by aggregation and decoupled from clay content. 7th International Symposium on Soil Organic Matter, 09.10.2019, Adelaide (Australien).

Schweizer, S. A., F. B. Bucka, M. Graf-Rosenfellner, I. Kögel-Knabner (2019): How clay content mediates the microaggregate composition and organic matter content of soils. Annual meeting of the German Soil Science Society (DBG), 26.08.2019, Bern (Switzerland).

Schweizer, S. A. (2019): Organic matter distribution along natural gradients: opportunities for the tropics. Amazonas and global change seminar, Land Surface Atmosphere Interactions (LSAI, TUM), 25.06.2019, Freising (Germany).

Schweizer, S. A., F. B. Bucka, M. Graf-Rosenfellner, I. Kögel-Knabner (2019): Impact of clay content on soil microaggregate arrangement and organic matter. EGU General Assembly, 10.4.2019, Vienna (Austria).

Schweizer, S. A., A. Koelbl, C. W. Mueller, C. Hoeschen, P. Ivanov, K. Eusterhues, I. Koegel-Knabner (2018): Organic matter accretion on soil mineral surfaces is decoupled from specific surface area. EGU General Assembly, 10.04.2018, Vienna (Austria)

Schweizer, S. A., C. Höschen, S. Schlüter, I. Kögel-Knabner, C. W. Mueller (2018): Microspatial patterns of organic matter accrual in microaggregates govern the rapid soil formation after glacial retreat. EGU General Assembly, 12.04.2018, Vienna (Austria)

Schweizer, S. A., A. Koelbl, C. Hoeschen, C. W. Mueller, I. Koegel-Knabner (2017): Microspatial distribution of soil organic matter coatings on mineral surfaces in arable Cambisols with a gradient in soil texture. Workshop on Formation, Properties and Function of Soil Microaggregates, 12.10.2017, Munich (Germany)

Schweizer, S. A., C. Höschen, S. Schlüter, A. Koelbl, I. Kögel-Knabner, C. W. Mueller (2017): Organic matter accrual at the microscale drives rapid soil structure formation after glacial retreat. Workshop on Formation, Properties and Function of Soil Microaggregates, 12.10.2017, Munich (Germany)

Schweizer, S. A., A. Koelbl, K. Eusterhues, P. Ivanov, C. Hoeschen, C. W. Mueller, I. Koegel-Knabner (2017): Assoziation organischer Bodensubstanz mit mineralischen Oberflächen in einem ackerbaulich genutzten Oberboden mit unterschiedlicher Bodentextur. Annual meeting of the German Soil Science Society (DBG), 04.09.2017, Göttingen (Germany)

Schweizer, S. A., S. Schlüter, C. Höschen, A. Koelbl, I. Kögel-Knabner, C. W. Mueller (2017): Quantifying the complex spatial arrangement of biogeochemical interfaces using NanoSIMS. NanoSIMS Usermeeting, 22.08.2017, Leipzig (Germany)

Schweizer, S. A., C. Hoeschen, S. Schlueter, I. Koegel-Knabner, C. W. Mueller (2017): Rapid soil structure formation after deglaciation through accrual of organic matter –an image analysis of elemental distributions by NanoSIMS. Goldschmidt, 16.08.2017, Paris (France)

Schweizer, S. A., A. Koelbl, C. Hoeschen, C. W. Mueller, I. Koegel-Knabner (2017): Soil texture mediates the biogeochemical association of soil organic matter with mineral surfaces in an arable Cambisol. Goldschmidt, 15.08.2017, Paris (France)

Schweizer, S. A., S. Schlüter, C. Höschen, I. Kögel-Knabner, C. W. Mueller (2017): Microscale soil structure development after glacial retreat – using machine-learning based segmentation of elemental distributions obtained by NanoSIMS. EGU General Assembly, 25.04.2017, Vienna (Austria)

Schweizer, S. A., A. Koelbl, C. Hoeschen, C. W. Mueller, I. Koegel-Knabner (2017): The association of soil organic matter with mineral surfaces depends on clay content in an arable Cambisol. EGU General Assembly, 24.04.2017, Vienna (Austria)

Schweizer, S. A., S. Tandy, B. Seitz, M. G. A. van der Heijden, R. Schulin (2016): Zinc and Cadmium in Soil and Wheat Grains on Swiss Farms: Comparison of Organic and Conventional Management. Annual Symposium World Food System Center (ETH), 04.11.2016, Zurich (Switzerland).

Schweizer, S. A., B. Seitz, S. Tandy, M. G. A. van der Heijden, R. Schulin (2016): Zinc and Cadmium in soil and grain on Swiss wheat farms: Comparison of organic and conventional management. Annual Spring Meeting of the Soil Science Society of Switzerland, 04.02.2016, Geneva (Switzerland).

Schweizer, S. A., B. Seitz, S. Tandy, M. G. A. van der Heijden, R. Schulin (2015): Zinc biofortification through organic matter management in Swiss wheat farms. rDay Institute of Terrestrial Ecosystems, 11.09.2015, Zurich (Switzerland).

Schweizer, S. A., M. Graf, N. A. Bhat, B. S. Sisodia, S. Zikeli, G. Cadisch, G. S. Bhullar (2015): Dynamische Bildanalyse von Bodenstrukturen unter einem Langzeitsystemvergleich biologischer und konventioneller Bewirtschaftung in Indien. Annual meeting of the German Soil Science Society (DBG), 08.09.2015, Munich (Germany).

Schweizer, S. A., N. A. Bhat, B. S. Sisodia, S. Zikeli, G. Cadisch, G. S. Bhullar (2015): Soil structure under a long-term system trial comparing organic and conventional management in India. Annual Conference of the Society for Tropical Ecology (GTÖ), 08.04.2015, Zurich (Switzerland).

Schweizer, S. A., N. A. Bhat, B. S. Sisodia, S. Zikeli, G. Cadisch, G. S. Bhullar (2014): Soil physical properties under a long-term system trial comparing organic and conventional management in India. Tropentag, 18.09.2014, Prague (Czech Republic).

G.3 Media contributions

Schweizer, S. (2014): How to fight food waste with disco music. Oral presentation. TEDxTUHH Beyond Conventions. Hamburg, Germany. https://youtu.be/aK9WfAn5NxI.

Schweizer, S., R. Schlumberger, A. Kurbasik (2014): Unter unseren Füßen. Bundesverband Boden e. V. video contest "Why is the forest soil important for us?". https://youtu.be/9CPJ0T2v8B8.